




# Sitosterol-rich *Digera muricata* against 7-ketocholesterol and lipopolysaccharide-mediated atherogenic responses by modulating NF-KB/iNOS signalling pathway in macrophages

Sangeetha Ravi<sup>1</sup> · Parimalanandhini Duraisamy<sup>1</sup> · Mahalakshmi Krishnan<sup>1</sup> · Livya Catherene Martin<sup>1</sup> · Beulaja Manikandan<sup>2</sup> · Manikandan Ramar<sup>1</sup> 

Received: 1 June 2023 / Accepted: 10 August 2023 / Published online: 3 September 2023  
© King Abdulaziz City for Science and Technology 2023

## Abstract

*Digera muricata* L., commonly known as Tartara, is an edible herb used as traditional medicine in many countries of Africa and Asia. This study aimed to elucidate the effect of a phytosterol-rich extract of *D. muricata* on 7-ketocholesterol-mediated atherosclerosis in macrophages. The extract was examined by phytochemical analyses, GC–MS, TLC, DPPH scavenging and hRBC membrane stabilization assays. Macrophage polarization was studied with experimental groups framed based on alamar blue cell viability and griess assays. Regulations of arginase enzyme activity, ROS generation, mitochondrial membrane potential, cell membrane integrity, pinocytosis, lipid uptake and peroxidation, as well as, intracellular calcium deposition were determined. In addition, expressions of atherogenic mediators were analysed using PCR, ELISA and immunocytochemistry techniques. Diverse phytochemicals with higher free radical scavenging activity and anti-inflammatory potential have been detected in the *D. muricata*. Co-treatment with *D. muricata* markedly reduced the atherogenic responses induced by 7KCh in the presence of LPS such as ROS, especially, NO and O<sub>2</sub><sup>-</sup> along with lipid peroxidation. Furthermore, *D. muricata* significantly normalized mitochondrial membrane potential, cell membrane integrity, pinocytic activity, intracellular lipid accumulation and calcium deposition. These results provided us with the potentiality of *D. muricata* in ameliorating atherogenesis. Additionally, it decreased the expression of pro-atherogenic mediators (iNOS, COX-2, MMP9, IL-6, IL-1β, CD36, CD163 and TGFβ1) and increased anti-atherogenic mediators (MRC1 and PPARγ) with high cellular expressions of NF-κB and iNOS. Results showed the potential of sitosterol-rich *D. muricata* as a versatile biomedical therapeutic agent against abnormal macrophage polarization and its associated pathologies.

**Keywords** Macrophages · Atherosclerosis · Phytosterol · 7-ketocholesterol · Cytokines

**Accession number:** The collected *Digera muricata* was taxonomically identified and confirmed by the Department of Botany, Alagappa University, Karaikudi, Tamil Nadu, India with a plant authentication certificate (Accession No: ALUH1832).

✉ Manikandan Ramar  
manikandanramar@yahoo.co.in

Sangeetha Ravi  
sangimaravi@gmail.com

Parimalanandhini Duraisamy  
parimalandhini.d@gmail.com

Mahalakshmi Krishnan  
mahalavanya1993@gmail.com

Livya Catherene Martin  
livyacatherene@gmail.com

## Introduction

Inflammation has been intensely investigated in the field of experimental medicine since the nineteenth century. It can be referred to as a restorative process with diverse cascades

Beulaja Manikandan  
beulaja@gmail.com

<sup>1</sup> Department of Zoology, University of Madras, Guindy Campus, Chennai 600 025, India

<sup>2</sup> Department of Biochemistry, Annai Veilankanni's College for Women, Chennai 600 015, India

of inflammatory responses which contains a series of reactions provided by cell and molecular activities in response to stimuli for tissue repair (Schmid-Schönbein 2006). While it is considered a complex contribution of the immune system to tissue healing and defensive processes, it is now regarded mainly for its adverse effects in the long run. Continuance of inflammation poses a great threat as it will lead to tissue damage, provoking chronic inflammation (Nathan and Ding 2010). The boon of technological developments has now increased human survival, resulting in the curse of chronic inflammation in all age populations. The persistence of chronic inflammations leads to several morbidities and mortalities in association with various inflammatory diseases, namely, rheumatoid arthritis, multiple sclerosis, neurodegenerative disorders, inflammatory bowel diseases and cardiovascular diseases (Punchard et al. 2004).

Cardiovascular diseases are the global cause of mortality, particularly in developing countries among which atherosclerosis remains a multifactorial life-threatening chronic inflammatory disorder that damages vital organs of the body, especially causing myocardial, claudication and cerebral infarctions. The cardiological society of India (CSI) has warned now India is the “chronic heart disease capital of the world” with a rising number of sudden cardiac death (SCD), especially among young adults. The current scenario with the COVID-19 pandemic terrifies worldwide and research indicates that it affects the vascular tissues resulting in atherosclerosis-linked mortalities. SARS-CoV-2 infection may either induce the manifestation of atherosclerosis or worsen the already existing endothelial dysfunction or atherosclerotic plaque (Vinciguerra et al. 2021). Recent advancements in the field of atherosclerosis have conveyed an evolution from the previous notions of its pathology. It is developed in the intimal layer of arteries which is influenced by the components of circulating blood. During early atherogenesis, endothelial cells lining the vascular tissues get activated upon stimulus and express several cell adhesion molecules (CAMs) on their surface and this phenomenon continues throughout the establishment of lesions (Swirski et al. 2006). This allows the circulating immune cells, monocytes/macrophages and leukocytes, to attach and extravasate into the intima influenced by obnoxious mediators in association with hypertension, diabetes and hyperlipidemia (Ross 1986, 1995; Frostegård 2013).

Atherosclerosis is majorly induced by the sequestration of apolipoprotein-B (apoB) containing cholesterol-rich low-density lipoproteins (LDL) which undergo oxidative, enzymatic or non-enzymatic modifications that lead to the activation of immune responses (Moore and Tabas 2011). Oxidation of cholesterol produces enormous oxidized LDL (Ox-LDL) byproducts also denoted as oxysterols. 7-ketocholesterol (7KCh) is one of the most abundant toxic Ox-LDL derivatives in atherogenic lesions, which are generally

formed through endogenous enzymatic reactions under oxidative stress (Anderson and Campo 2020; Mahalakshmi et al. 2021). It is produced when the fatty acid esters of cholesterol undergo auto-oxidation that is found to exert cytotoxic and apoptotic effects with the most atherogenic nature, thereby distressing intracellular homeostasis (Ravi et al. 2021). 7KCh induces various cellular damages through endoplasmic reticulum stress along with epidermal growth factor receptor (EGFR) and toll-like receptor-4 (TLR4) activation. TLRs are the leading cause of the pathogenesis of cardiovascular diseases, especially atherosclerosis which can be experimentally induced using bacterial lipopolysaccharide (Huang et al. 2010; Roshan and Tambo 2016).

Lipopolysaccharide (LPS) is one of the major components of Gram-negative bacterial cell walls. The endotoxin bagged by the lipoprotein may give rise to inflammation after the fusion of lipoprotein into the vascular wall (Ostos et al. 2002). LPS stimulates endothelial cells to undergo diverse cellular responses through the upregulation of pro-inflammatory cytokines, growth factors and adhesion molecules (Bannerman and Goldblum 2003). It was also proposed that increased LDL oxidation upon LPS administration also promotes atherogenesis through macrophages. 7KCh has been proven to be accountable for modulating macrophages by converting their phenotype from anti-inflammatory to pro-inflammatory subtype (Berthier et al. 2005; Larsson et al. 2007; Buttari et al. 2013).

Macrophages are mononuclear phagocytes and the most prominent innate immune cell found to be involved in the pathophysiology of atherosclerosis. They are matured forms of recruited monocytes that further multiply upon stimuli-like macrophage colony-stimulating factors (MCSFs). Certain characteristic features including their heterogeneity and plasticity are recently found to play an important role in atherogenesis (Libby et al. 2009). They undergo ingestion of accumulated modified LDL and transform into lipid-engorged foam cells that persist in the plaque, prompting the disease to progress. This type of macrophage phenotype alteration owing to lipid dysregulation compromises the beneficial clearance response into a deleterious sequence (Moore et al. 2013). Macrophages exhibit a wide spectrum of phenotypic subsets, namely, M1, M2, M3, M4 and Mhem among which M1 and M2 are well described to be regulating inflammatory responses during atherogenesis (Chinetti-Gbaguidi et al. 2015). M1 macrophages are classically activated upon stimuli, especially lipoproteins, engaging in tissue destruction and secretion of pro-inflammatory cytokines (Interleukin (IL)-1 $\beta$ , IL-6 and Tumour necrosis factor (TNF)- $\alpha$ ), chemokines, enzymes (matrix metalloproteinase (MMP)-9 and cyclooxygenase (COX)-2) as well as additionally produce ROS/RNS (Martinez et al. 2006; Mosser and Edwards 2008; Xue et al. 2014). On the contrary, M2 macrophages are alternatively activated and

display anti-inflammatory properties by producing IL-10, mannose receptor C-type 1 (MRC1), peroxisome proliferator-activated receptor gamma (PPAR $\gamma$ ) and extracellular matrix components (ECM) such as collagen for tissue repair (Barrett 2020; Duraisamy et al. 2022). M2 phenotypic macrophages orchestrate the resolution of inflammatory response at the site of atherogenesis. Maintaining a dynamic balance of M1 and M2 macrophages is crucial to undergo proper inflammation. Recent studies are evidence that an imbalance in these macrophage ratios due to the phenotypic switch from M2 to M1 primes atherosclerotic lesion development (Khallou-Laschet and Varthaman 2010). This detrimental phenotypic shift is influenced by 7KCh which impairs the resolution properties of M2 macrophages such as increased loading of Ox-LDL by opposing the cholesterol efflux mechanisms (Gelissen et al. 1996). In addition, oxidative stress through reactive oxygen species (ROS) is significantly induced along with cell cycle arrest and apoptosis in macrophages upon exposure to 7KCh (Palozza et al. 2010).

The pro-oxidant action of 7KCh and related oxysterols results in an oxidative burst by macrophages with excessive levels of ROS/RNS especially, nitric oxide (NO) and superoxide anion ( $O_2^-$ ) under the primary effect of a spectrum of enzymes such as nicotinamide adenine dinucleotide phosphate (NADPH)-oxidase, nitric oxide synthases (NOS), xanthine oxidase and mitochondrial enzymes (Leonarduzzi et al. 2006; Li and Horke 2014). NO is found to be one of the critical moderators of diseases associated with vascular tissues synthesized by inducible NOS (iNOS). A variety of physiological as well as inflammatory mechanisms is mediated by NO during atherogenesis, namely, endothelial dysfunction, vasorelaxation, adhesion of platelet as well as leukocyte chemotaxis inhibition (Napoli and Ignarro 2001; Napoli et al. 2006). NO is one of the specific markers for M1 phenotype macrophages and the coupling of NO with  $O_2^-$  forms an unstable reactive pro-oxidant molecule, peroxynitrite ( $ONOO^-$ ). These reactive gaseous molecules in surplus facilitate toxic reactions during atherogenesis, especially, the oxidation of cholesterol as well as peroxidation of membrane lipids which is dependent on  $ONOO^-$  (Rubbo et al. 1994; Patel et al. 2000; Förstermann et al. 2017).

Current therapeutics for atherosclerosis include LDL-cholesterol-lowering therapies (HMG-CoA reductase inhibitors, cholesterol absorption inhibitors, xestin type-9 inhibitors, bile acid sequestrates), triglycerides-lowering therapies (statins, fibrates, n-3 fatty acids) and HDL-cholesterol-increasing therapies (cholesterol ester transfer protein (CETP) inhibitors) (Bergheanu et al. 2017). Long-term consumption of such steroidal and non-steroidal formulated drugs largely leads to an increased risk of developing concomitant side effects and this brings in a prerequisite

to unfold better alternatives in particular, cardio-protective plant-based drugs that are devoid of such deleterious effects.

*Digera muricata*, also known as Tartara, is a widely distributed edible medicinal tropical plant in several countries of Africa and Asia such as Kenya, Sudan, South Ethiopia, Tanzania, Yemen, India, Pakistan, Malaysia, etc. It is a coolant, astringent and laxative in Ayurveda and rich in micronutrients with wide distribution (Mathad and Mety 2010; Ghaffar et al. 2019). Several studies support the competent anti-oxidant effect of *D. muricata* on oxidative stress by decreasing thiobarbituric acid reactive substances (TBARS) which are byproducts of lipid peroxidation with correspondingly increasing levels of enzymes namely, superoxide dismutase, peroxidase, catalase, glutathione peroxidase (GPx), quinone reductase (QR), glutathione-S-transferase (GST) and reduced glutathione providing evidence for free radical scavenging activity (Khan and Ahmed 2009; Khan et al. 2009; Muhammad et al. 2011). The protective effect of *D. muricata* was accredited by attenuating the altered biochemical mediators, DNA fragmentation and inhibiting telomerase activity (Khan et al. 2009; Khan and Younus 2011). In addition, the significant reduction of gamma-glutamyltransferase ( $\gamma$ -GT) and malondialdehyde (MDA) upon methanol extract of *D. muricata* warrants its efficiency in cytoprotection (Khan et al. 2011a, b). The methanol extract of *D. muricata* was investigated for its active anti-inflammatory, anti-microbial and anti-diabetic activities (Jagatha and Senthilkumar 2011; Miah et al. 2017; Ramalashmi 2019; Patel Shivani and Nainesh 2017; Shah et al. 2020). It is evident from the recent exploration of the biomedical properties expressed by *D. muricata* that its methanol leaf extract may potentially be ideal for preventing the polarization of macrophages and atherogenesis. Hence, in this study, we elucidated for the first time, the anti-atherogenic potential of *D. muricata* methanol leaf extract against 7KCh and LPS-induced polarization of M2 phenotypic IC-21 macrophages in vitro.

## Materials and methods

### Collection and identification of plant material

Fresh *Digera muricata* (Thoiya keerai in Tamil) plants belonging to the Amaranthaceae family were collected around the cultivation field of Kancheepuram district, Tamil Nadu, India. The collected plant was taxonomically identified and confirmed by the Department of Botany, Alagappa University, Karaikudi, Tamil Nadu, India with a plant authentication certificate (Accession No: ALUH1832). Fresh leaves were collected from the plant, washed thoroughly with water, air dried to remove the moisture content at room

temperature, pulverized into a fine powder and stored in an airtight container until further studies.

### Preparation of sitosterol-rich fraction from *D. muricata*

Air-dried leaf powder of *D. muricata* was subjected to extraction by following the method of Gulluce et al. (2007) with methanol as a solvent source using a Soxhlet extractor for 72 h at a temperature of 40 °C, less than the boiling point of methanol. The resultant plant-solvent extract was filtered using Whatman filter paper No. 1 and air-dried at room temperature for evaporation of the solvent. The following residual extract was stored and maintained in a dry, cold condition until further experiments.

### Phytochemical analysis

The prepared *D. muricata* leaf extract was subjected to qualitative analyses followed by methods of Daniel and Krishnakumari (2015) and Geetha and Geetha (2014) for diverse bioactive phytochemicals, namely, saponins, tannins, alkaloids, reducing sugars, flavonoids, glycosides, steroids, terpenoids and phenols. The methods followed for the qualitative analyses of each of the aforementioned phytochemicals have been mentioned in Table 1.

### Thin-layer chromatography (TLC) profiling of the crude extract

TLC analytical profiling was performed by following the modified method of Pascual et al. (2002). In brief, a silica gel 60 F<sub>254</sub>-coated TLC plate (Merck, Chemical Ltd, India) was acquired for the stationary phase. Leaf extract of *D. muricata* was spotted on a TLC plate and solvent systems with different ratios of hexane, ethyl acetate, chloroform and methanol were used as a mobile phase until proper band resolution. The chromatograms were then visualized under visible light, short UV (254 nm) and long UV (365 nm) without any chemical treatment and retention factors ( $R_f$ ) were calculated for each band observed.

### Gas chromatography-mass spectroscopic analysis of *D. muricata* leaf extract

Leaf extract of *D. muricata* had been analysed for the presence of bioactive phytochemicals using GC-MS (Gomathi et al. 2015) Agilent GC 7890A/MS5975C GC-MS instrument consisting of Agilent DB5MS capillary column with specifications of 30 m/0.25 mm internal diameter/ 0.25- $\mu$ m film thickness was utilized to characterize the extract. The

sample was analysed for a run time of 23.833 min with the oven program reaching upto 300 °C. The obtained retention index data and gas chromatographic profile were compared with the National Institute of Standards and Technology (NIST) library.

### Analysis of free radical scavenging activity using DPPH

2,2-diphenyl-1-picryl-hydrazyl-hydrate (DPPH) is a stable free radical that estimates the free radical scavenging activity of antioxidants. The reaction DPPH solution was prepared for 0.3 mM with methanol freshly in regard to its radical instability. The free radical scavenging activity was estimated by following the method of Brand-Williams et al. (1995) with modifications. 1 ml of leaf extract at different concentrations (25–400  $\mu$ g/ml) was added to 0.5 ml of 0.3 mM DPPH methanol solution in test tubes and the experimental setup was incubated in a dark environment at room temperature for 30 min. Following incubation, the optical density of the reaction mixture was recorded using a UV-visible spectrophotometer at 517 nm. Ascorbic acid was used as a standard antioxidant and the percentage of scavenging activity was calculated. The level of DPPH free radical scavenging activity was expressed in terms of the percentage of reduction (%).

### Determination of anti-inflammatory activity using hRBC membrane stabilizing assay

The anti-inflammatory property of various concentrations of *D. muricata* leaf extract was determined by performing a human red blood cell (h)RBC membrane stabilizing assay as described by Madhu et al. (2014) with modifications. Fresh blood was collected from a healthy donor in a sterile solution, the packed cells were obtained and washed thrice with isosaline (0.9%) to remove any bound serum protein. A stock hRBC suspension of 10% v/v was prepared with 10 mM phosphate-buffered saline. The reaction mixture was prepared with 1 ml of leaf extract at different concentrations (25–400  $\mu$ g/ml) made up of 10 mM PBS, 2 ml of hyposaline (0.25% NaCl) along with 0.5 ml of stock hRBC suspension. Hyposaline was substituted with distilled water in the control tube. The experimental setup was incubated for 30 min at 37 °C followed by centrifugation for 20 min. Dexamethasone (400  $\mu$ g/ml) is steroidal standard anti-inflammatory drug commercially used, and hence, it was taken as a standard drug. At the end of the experiment, the optical density of the supernatant was assessed at a wavelength of 560 nm using a UV-Vis spectrophotometer and the inhibition of hemolysis was expressed as absorbance with optical density (OD).

## Culture of IC-21 macrophage cell line

The immortalized IC-21 macrophage cell line was procured from National Center for Cell Science (NCCS), Pune. IC-21 macrophages were ideal for this experimentation as they were identified to express M2 phenotype with non-inflammatory characteristics under cultured conditions (Lopukhov et al. 2021; Smythe et al. 2003). Cells were cultured and maintained under optimal culture conditions of 5% CO<sub>2</sub> at 37 °C in a humidified incubator with RPMI-1640 (Roswell Park Memorial Institute) medium supplemented with 10% fetal bovine serum (FBS) and 1% antibiotic solution. On attaining confluency, cells were passaged using 1X PBS (phosphate buffered saline; pH: 7.4) and were utilized for further experiments.

## Determination of cell viability using alamar blue and observation of cytomorphology

The viability of IC-21 macrophages upon treatment with test components at different concentrations was assessed with alamar blue dye. The aim of this experiment was to determine the optimal concentrations for carrying out further experimental studies with maximum viability. Macrophages were treated with different concentrations of 7KCh (2, 4, 6, 8 and 10 µg/ml), LPS (25, 50, 100, 200 and 400 ng/ml) and *D. muricata* leaf extract (25, 50, 100, 200, 400, 600, 800 and 1000 µg/ml), respectively, for a period of 24 h. The treated cells after experimental time were incubated with 0.1% alamar blue for 5 h at a standard culture condition of 5% CO<sub>2</sub> at 37 °C and changes in the optical densities of the treated cells were monitored at 570 and 600 nm for the oxidized and reduced forms of alamar blue, respectively. The percentage (%) of cell viability was calculated using the standard formula (O'Brien et al. 2000). Simultaneously, cells were observed under a phase contrast microscope (Nikon) for the visual assessment of their impact on macrophage cytomorphology.

## Estimation of nitric oxide using Griess reagent

The nitric oxide (NO) level in the form of nitrite was quantified by a colorimetric assay using Griess reagent with modifications (Yang et al. 2009). Following treatment of IC-21 macrophages with test components, culture supernatants were retrieved for measurement of NO. At the end of the experimental time periods, 50 µl of culture supernatant was mixed with 50 µl of 0.1% NED and 50 µl of 1% sulfanilamide. The reaction mixture was incubated for 20 min at room temperature in dark and the absorbance was measured at 540 nm. NO generation in the treated cells was calculated

using the standard graph of sodium nitrite and expressed in concentrations (µM). Initially, the NO level was measured for different concentrations of 7KCh (2, 4, 6, 8 and 10 µg/ml) and LPS (25, 50, 100, 200 and 400 ng/ml) at different time intervals (1–5 h and 24 h). From this experiment, one significant concentration for 7KCh (8 µg/ml) and LPS (200 ng/ml) was selected and experimental groups were framed as follows:

Group I:	Cells were incubated with RPMI-1640 medium containing 0.5% FBS for 24 h
Group II:	Cells were treated with 8 µg/ml of 7KCh for 24 h
Group III:	Cells were treated with 8 µg/ml of 7KCh and 200 ng/ml of LPS for 24 h
Group IV:	Cells were treated with 8 µg/ml of 7KCh, 200 ng/ml of LPS and different concentrations (25, 50, 100, 200 and 400 µg/ml) of leaf extract of <i>D. muricata</i> for 24 h

Furthermore, NO levels produced upon treatment of the above-given experimental setup were also estimated. It must be noted that the assay was carried out entirely in RPMI-1640 medium containing only 0.5% FBS as serum proteins are speculated to interfere with the OD values recorded at the end of the experiment.

## Estimation of arginase enzyme activity

Arginase enzymatic activity was estimated in cell lysates following the method of Munder et al. (2005) with slight modifications. In concisely, 100 µl cell lysate was added with 20 µl of 10 mM MnCl<sub>2</sub> and heated (10 min) for activating the enzyme. 100 µl of 0.5 M L-arginine was added and incubated for 15–75 min at 37 °C, followed by ending the reaction with 900 µl of H<sub>2</sub>SO<sub>4</sub>: H<sub>3</sub>PO<sub>4</sub>: H<sub>2</sub>O (1: 3: 7). Urea concentration was measured at 540 nm after heating the reaction mixture with 40 µl α-isonitrosopropiophenone at 95 °C for 30 min. The enzyme activity is expressed in terms of urea concentration (M) with commercial urea as the standard.

## Analysis of pinocytic activity by neutral red uptake method

Neutral red is a vital dye endocytosed by macrophages into their lysosomes by the process of pinocytosis. The pinocytic activity of IC-21 macrophages was analysed by neutral red uptake by following the method of Al Obaydi et al. (2020) with modifications. IC-21 macrophages were treated with different experimental groups as mentioned above for a period of 24 h. After treatment, macrophages were incubated with 100 µl of 0.75% neutral red for 2 h. Cells were then

washed and lysed with 100  $\mu$ l of cell lysis solution (acetic acid and ethanol at a 1:1 ratio) and incubated overnight. The absorbance was measured at 540 nm, and the relative activity was expressed as optical density values (OD).

### Estimation of lipid accumulation using oil red O assay

Lipid accumulation in the cells was quantified by staining with lipid-specific oil red O followed by the method of Kraus et al. (2016). Cells were treated according to experimental groups for 24 h. After treatment, cells were washed with 1X PBS, followed by fixation with 10% NBF for 20 min at room temperature and further washing with 1X PBS. 500  $\mu$ l of oil red O working stain solution was added to each well and incubated for 30 min at room temperature. The stain was removed after incubation and cells were washed with distilled water to remove excess stain. To elute the stain from the cells, 100% isopropanol is added to the cells and incubated for 10 min. The absorbance of eluted stain was measured at 510 nm using a spectrophotometer and expressed as optical density values (OD).

### Assessment of lipid peroxidation using thiobarbituric acid (TBA)

Thiobarbituric acid reactive substances (TBARS) which are biomarkers of oxidative stress and lipid oxidation during atherogenesis were assessed using TBA reagent according to the protocol of Utley et al. (1967) with modifications. In brief, following the experimentation, cells were lysed with cell lysis buffer and the supernatant was collected. To 0.5 ml of the supernatant, 2 ml of 20% TCA and 4 ml of 0.67% TBA were mixed and boiled for 10 min. The mixture was then centrifuged for 10 min at 4 °C and the optical density of the supernatant was measured at 530 and 600 nm. The activity was expressed in nmoles.

### Qualitative and quantitative assessment of ROS generation in macrophages

Estimation of intracellular ROS was performed using a cell-based dichlorodihydrofluorescein diacetate (DCFH-DA) dye assay qualitatively as well as quantitatively following the method of Tiwari et al. (2010). Macrophages were treated with test compounds for 24 h and at the end of the incubation period, the existing medium was removed and washed with serum-free medium gently. 100  $\mu$ l of dissolved 0.1% DCFH-DA was overlaid on the coverslips and incubated for 30 min in the incubator. The incubated cells were observed using a Carl Zeiss confocal fluorescent microscope for

qualitative examination. To quantify the level of ROS generation, the incubated cells were lysed with ethanol: acetic acid (1:1). The fluorescence was measured using a spectrofluorometer at excitation 485 nm and emission 530 nm and expressed as optical density values (OD).

### Determination of intracellular superoxide anion ( $O_2^-$ ) generation using NBT assay

Estimation of intracellular  $O_2^-$  generation was performed quantitatively using nitroblue tetrazolium chloride (NBT) following a modified colorimetric method (Sim Choi et al. 2006). After experimentation of different groups, cells were incubated with 100  $\mu$ l of NBT solution for 1 h. At the end of incubation, cells were washed twice with PBS followed by once with methanol and air-dried to remove the extracellular dye solution. The intracellular deposited NBT was dissolved with 120  $\mu$ l of KOH and 140  $\mu$ l of DMSO. The intensity of the blue colour indicated the level of superoxide anion present in them. Their absorbance was measured at 620 nm and expressed as optical density values (OD).

### Localization of mitochondria using rhodamine 123/ DAPI staining method

The mitochondrial membrane potential of experimented IC-21 macrophages was analysed using rhodamine 123 (Rh123) fluorescent dye following the methodology of Johnson et al. (1980) with modifications. 4',6-diamidino-2-phenylindole (DAPI) was used as a counter stain for the nucleus. In brief, macrophages were treated with different experimental groups and stained initially with rhodamine 123 (1 mg/ml in serum-free medium) for 20 min. Following this, DAPI dye was added to the cells and further incubated for 5 min in dark at room temperature. After incubation, cells were washed gently with serum-free medium to remove excess stain and mounted on glass slides for observation under a Carl Zeiss confocal fluorescent microscope.

### Determination of cellular membrane integrity using acridine orange-ethidium bromide staining

The membrane integrity of macrophages was examined using acridine orange and ethidium bromide (AO/EB) staining assay (Peng et al. 2020). After treatment, the experimental groups were stained with AO/EB stains (1 mg/ml in serum-free medium) and incubated for 5 min at room temperature. Following incubation, cells were gently washed with serum-free medium and observed under a Carl Zeiss confocal fluorescent microscope. Macrophages

were then categorized into live cells (L), early apoptotic cells (EA) and late apoptotic cells (LA).

### Quantification of intracellular calcium deposits using alizarin red S (ARS) staining method

Intracellular calcium deposits were evaluated using an anthraquinone dye, alizarin red S. Calcified minerals are extracted from the experimental groups for assessing mineralization at low pH (Gregory et al. 2020). After treatment, the medium was removed and macrophages were washed with 1X PBS. They were then fixed with 10% NBF for 20 min at room temperature. 200 µl of 40 mM alizarin red S dye was added and incubated for 30 min at room temperature. After incubation, the dye was removed and cells were washed with 1X PBS followed by incubation for 30 min with 10% acetic acid for stain extraction. The solubilized stain resulted in a colour change from red to yellow due to acidic pH. The optical density of extracted stain was measured at 405 nm in a well plate reader and expressed as optical density values (OD).

### Isolation of total RNA, RT-PCR and target sequence amplification

The gene expression analysis of pro-atherogenic and anti-atherogenic mediators was conducted with extract of *D. muricata* by following the method of Manikandan et al. (2020). After treatment, cells were harvested and pelleted. Pellets were processed for the isolation of total cellular RNA. Subsequently, cell lysate was prepared with calculated volumes of trizol (100 µl/10 mg) and incubated for 10 min with an equal volume of ice-cold chloroform at room temperature. Following this, the sample was vortexed briefly, centrifuged at 12,000 rpm for 20 min at 4 °C and the supernatant was again centrifuged with ice-cold isopropanol in a 1: 2.5 ratio. The resulting pellet was ethanol precipitated and reverse transcribed into cDNA using Thermo Scientific First-strand cDNA synthesis kit. Primers spanning exon-exon boundaries were designed using NCBI Primer-BLAST program for some of the atherogenic and anti-atherogenic markers. The primer sequences are presented below.

Target gene	Primer sequences
iNOS	CCAAGTACGAGTGGTTCCAGG (FP) GTCCTCCAGGGCTCGATCTG (RP)
IL-1β	CTTTGAAGAAGAGCCCATCCT (FP) TCTGCTTGTGAGGTGCTGATG (RP)
IL-6	TTCACAGAGGATACCACTCCC (FP) GTGACTCCAGCTTATCTCTTG (RP)
MMP-9	CTTCAAGGACGGTTGGTACTG (FP) CAAGTCGAATCTCCAGACACG (RP)

Target gene	Primer sequences
COX-2	GGAAAAGGTTCTTCTACGGAG (FP) CCACCAATGACCTGATATTTC (RP)
CD36	TGAATGGTTGAGACCCCGTG (FP) CGTGGCCCGGTTCTACTAAT (RP)
CD163	GGAGTGACCTGCTCAGATGG (FP) TGTCACACCAGCGTCTTCTC (RP)
MRC1	TCCCGCTGGGTGTCAGATTC (FP) TCTCGCTTCCCTCAAAGTGC (RP)
PPARγ	CGAGTGTGACGACAAGGTGA (FP) GCCCAAACCTGATGGCATTG (RP)

About 100 ng of cDNAs was utilized for amplification. PCR-amplified products were then separated through the agarose gel electrophoresis technique and visualized under UV light for target gene amplification. The level of gene amplification was quantified using ImageJ densitometric analysis and expressed in terms of density with arbitrary units (a.u).

### Enzyme-linked immunosorbent assay of TGFβ1

The concentration of transforming growth factor β1 (TGFβ1) in the cell culture medium was estimated by ELISA (Xin et al. 2019). The culture medium was collected after 24 h and centrifuged at 800 rpm for 5 min. The sample was analysed using a TGFβ1 ELISA kit (Elabscience, Wuhan, China) following the manufacturer's protocol. In brief, the sample was activated and incubated with primary antibodies coated in the well plate, followed by incubation with a biotinylated detection antibody and HRP conjugate. A substrate for the reaction was added and measurement was observed at 450 nm. After quantification of TGFβ1 concentration, the levels were expressed in ng/ml.

### Immunocytochemistry analysis of pro-atherogenic mediators

Expressions of nuclear factor kappa B (NF-κB) and iNOS in macrophages were observed using the immunocytochemistry technique following the method of Yan et al. (2016). Following 24 h of treatment, cells were fixed with 10% neutral buffered formalin for 10 min. Membrane permeability was induced with 0.1% triton X-100 and blocked with 5% BSA blocking buffer for 2 h. Cells were incubated with primary antibodies in 1% BSA-TBST at 4 °C for 3 h after which FITC-conjugated secondary antibody was added and incubated for 2 h. 100 µl of DAPI was added for 5 min to stain the nucleus and the cells were observed under a confocal fluorescent microscope (Carl Zeiss ApoTome.2, Germany).

## Statistical analysis

The statistical significance was assessed using GraphPad Prism (version 8.4.2) software. The comparison between different groups was performed with a student *t*-test (Bryman and Cramer 2012).

## Results

### Phytochemical composition of *D. muricata* leaf extract

Phytochemical analyses of *D. muricata* leaf extract revealed the presence of biologically active phytochemicals such as saponins, tannins, alkaloids, reducing sugars, flavonoids, steroids, terpenoids, glycosides and phenols. The level of their presence/absence is given in Table 1.

### Thin-layer chromatography (TLC) profiling of the crude extract

Thin-layer chromatography profiling for visualization of possible secondary metabolites in the crude extract showed the presence of several phytochemicals. After trying out different combinations of solvents (hexane, ethyl acetate, chloroform and methanol), the ideal separation profile of compounds was achieved with hexane: ethyl acetate at the ratio of 8.4:1.6. Under the observation of visible light, short UV and long UV illumination, a total number of nine bands were observed which included eight bands under visible light (Fig. 1A), a purple band under short UV (Fig. 1B) and a fluorescent band under long UV

(Fig. 1C). The band profile and their respective retention factors ( $R_f$ ) have been calculated and displayed (Fig. 1).

### Gas chromatography-mass spectroscopic analysis of *Digera muricata* leaf extract

In order to find out the possible bioactive compounds, the extract of *D. muricata* was subjected to GC–MS analysis (Fig. 2). The chromatogram indicated the retention time and the abundance of each of the compounds present in the extract. The difference in the peak area can be observed with respect to the peak height. The compounds present in the extract along with their retention time (RT), quality, peak area (%), molecular weight (MW), molecular formula and their reported properties have been provided in the table (Table 2). The result showed the presence of 20 compounds with majorly

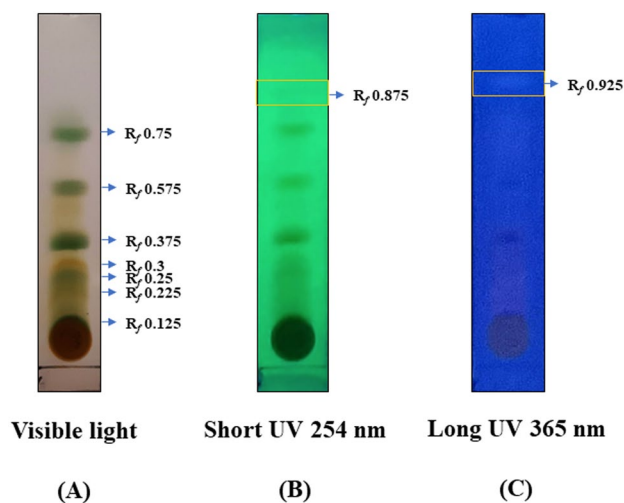


**Fig. 1** Thin layer chromatogram profile of *Digera muricata* leaf extract visualized under different light sources. **A** Visible light; **B** Short UV at 254 nm and **C** long UV at 365 nm

**Table 1** Phytochemical analysis of *Digera muricata* extract

S. no	Phytochemicals constituents	Test performed	<i>Digera muricata</i> methanol leaf extract
1	Saponins	Foam test	+
2	Tannins	Ferric chloride test	++
3	Alkaloids	Wagner's test	+++
4	Reducing Sugars	Fehling's test	+
5	Flavonoids	Lead-acetate test	+++
6	Glycosides	Keller Kiliani test	+
7	Steroids	Liebermann–Buchard test	+++
8	Terpenoids	Salkowski test	++
9	Phenols	Ferric chloride test	++

Data represent concordant values obtained from three determinations

+++ = indicates higher presence, ++ = indicates moderate presence, + = indicates low presence, – = indicates absence



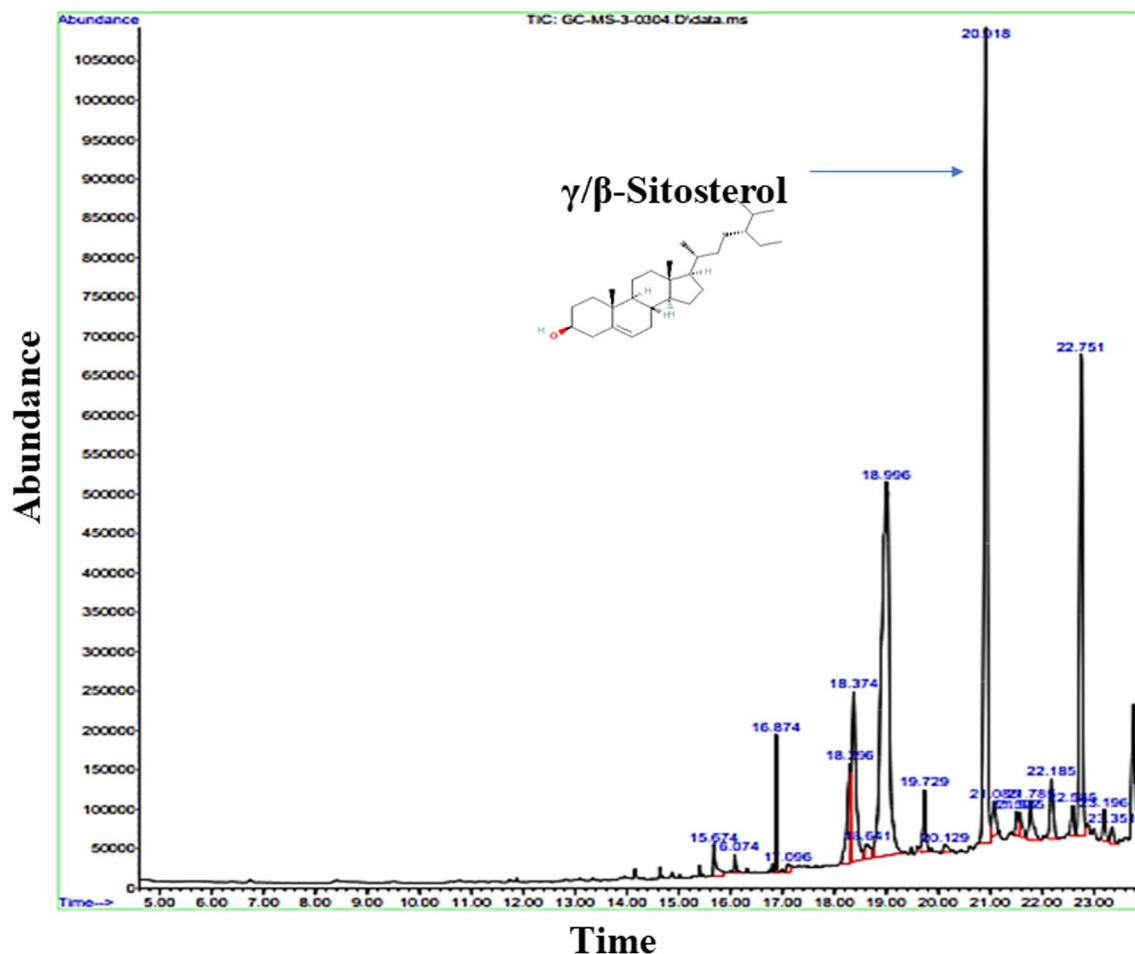


**Fig. 2** Gas chromatography–mass spectrometry chromatogram analysis of *Digera muricata* leaf extract

of  $\gamma$ -sitosterol (31.23%) along with other bioactive compounds, namely 4H-1,3,2-dioxaborin, 6-ethenyl-2-ethyl-4-methyl-4-(2-methylpropyl)- (27.29%) and stigmast-4-en-3-one (15.32%) covered major peak areas. Other anti-inflammatory and anti-atherogenic compounds like *n*-hexadecanoic acid, phytol, *cis*-vaccenic acid, lariciresinol, stigmasta-3,5-dien-7-one and  $\beta$ -sitosterol acetate were also found. The presence of phytosterols such as  $\gamma$ -sitosterol and stigmast-4-en-3-one in the leaves of *D. muricata* is first reported in this study.

### Free radical scavenging activity of *Digera muricata* leaf extract using DPPH

DPPH radical was analysed to be scavenged efficiently by the reference control (L. Ascorbic acid) and *D. muricata* leaf extract even at the lowest tested concentration of 25  $\mu\text{g/ml}$ . This activity was found to be concentration-dependent when tested linearly upto the highest concentration of 400  $\mu\text{g/ml}$  (Fig. 3). The scavenging activity of the

extract was almost equal to the standard with a high radical scavenging percentage.

### Anti-inflammatory effect of *Digera muricata* leaf extract using hRBC membrane stabilizing activity

The membrane stabilizing effect of *D. muricata* leaf extract on human RBC upon exposure to a hypotonic solution was determined to assess its anti-inflammatory property. The maximum membrane stability was exhibited by the highest concentration of tested extract. Comparatively, an effective membrane stabilization potential was observed even at the lowest concentration of 25  $\mu\text{g/ml}$ . A dose-dependent increase in membrane stabilization activity was exerted by *D. muricata* leaf extract up to the highest tested concentration of 400  $\mu\text{g/ml}$  (Fig. 4). Differences in the optical densities obtained for dexamethasone and different concentrations of *D. muricata* leaf extract were significantly decreased ( $*p < 0.05$  and  $**p < 0.01$ ) when compared to the tested control.

**Table 2** GC–MS analysis of *D. muricata* extract

S. no	Compound	RT	Quality	Peak area %	MW	M. formula	Properties reported
1	<i>n</i> -Hexadecanoic acid	15.674	83	1.02	256.4241	C <sub>16</sub> H <sub>32</sub> O <sub>2</sub>	Anti-inflammatory
2	Tridecanoic acid	16.074	53	0.35	214.34	C <sub>13</sub> H <sub>26</sub> O <sub>2</sub>	Antimicrobial
3	Phytol	16.874	90	1.50	296.5310	C <sub>20</sub> H <sub>40</sub> O	Anti-inflammatory
4	<i>Cis</i> -Vaccenic acid	17.096	95	0.32	282.4614	C <sub>18</sub> H <sub>34</sub> O <sub>2</sub>	Anti-inflammatory
5	2-Ethoxy-4-anisaldehyde	18.296	38	3.82	180.20	C <sub>10</sub> H <sub>12</sub> O <sub>3</sub>	Volatile organic compound
6	Cyclohexyldeimethylsilyloxybenzene	18.374	38	7.35	233.38	C <sub>10</sub> H <sub>23</sub> NO <sub>3</sub> Si	Silylating agent
7	2(3H)-Furanone, dihydro-3,4-bis[(4-hydroxy-3-methoxyphenyl)methyl]-, (3R-trans)-	18.641	64	0.91	358.39	C <sub>20</sub> H <sub>22</sub> O <sub>6</sub>	Lignan
8	4H-1,3,2-Dioxaborin, 6-ethenyl-2-e thyl-4-methyl-4-(2-methylpropyl)-	18.996	38	27.29	208.11	C <sub>12</sub> H <sub>21</sub> BO <sub>2</sub>	Antifungal
9	Hexadecanoic acid, 2-hydroxy-1-(hydroxymethyl) ethyl ester	19.729	62	1.66	330.5026	C <sub>19</sub> H <sub>38</sub> O <sub>4</sub>	Anti-inflammatory
10	(+)-Lariciresinol	20.129	92	0.41	360.4	C <sub>20</sub> H <sub>24</sub> O <sub>6</sub>	Anti-atherosclerotic
<b>11</b>	<b>γ/β-Sitosterol</b>	<b>20.918</b>	<b>95</b>	<b>31.23</b>	<b>414.7078</b>	<b>C<sub>29</sub>H<sub>50</sub>O</b>	<b>Anti-atherosclerotic</b>
12	6-Nitro-1-tryptophan	21.085	25	1.26	249.22	C <sub>11</sub> H <sub>11</sub> N <sub>3</sub> O <sub>4</sub>	Inhibitor of rhIDO
13	2- <i>t</i> -Butyl-6-methyl-5-(1-phenylbut-3-enyl)[1,3] dioxan-4-one	21.507	51	0.80	302.4	C <sub>19</sub> H <sub>26</sub> O <sub>3</sub>	NA
14	Cyclopropanecarboxylic acid, hydrazide, N2-cyclooctylideno	21.585	38	0.60	208.3	C <sub>12</sub> H <sub>20</sub> N <sub>2</sub> O	NA
15	Naphthalene, 1,1'-methylenebis-	21.785	62	1.61	268.3517	C <sub>21</sub> H <sub>16</sub>	NA
16	Stigmasta-3,5-dien-7-one	22.185	89	2.14	410.7	C <sub>29</sub> H <sub>46</sub> O	Anti-inflammatory
17	β-Sitosterol acetate	22.585	30	0.92	456.7434	C <sub>31</sub> H <sub>52</sub> O <sub>2</sub>	Anti-inflammatory
18	Stigmast-4-en-3-one	22.751	99	15.32	412.7	C <sub>29</sub> H <sub>48</sub> O	Anti-inflammatory
19	9,10-Methanoanthracen-11-ol, 9,10-dihydro-9,10,11-trimethyl	23.196	60	0.93	250.3	C <sub>18</sub> H <sub>18</sub> O	Anti-microbial
20	Carbamic acid, 4-methoxyphenyl-, allyl ester	23.351	58	0.56	207.23	C <sub>11</sub> H <sub>13</sub> NO <sub>3</sub>	NA

The value in bold signifies the extract is rich in sitosterol to support the given title

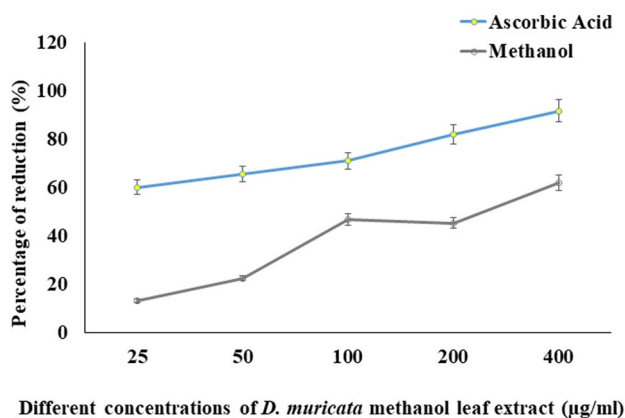


**Fig. 3** Free radical scavenging activity of *Digera muricata* leaf extract determined using DPPH assay with ascorbic acid as a standard reference at different concentrations (µg/ml). Each data represent the mean ± SD of three determinants

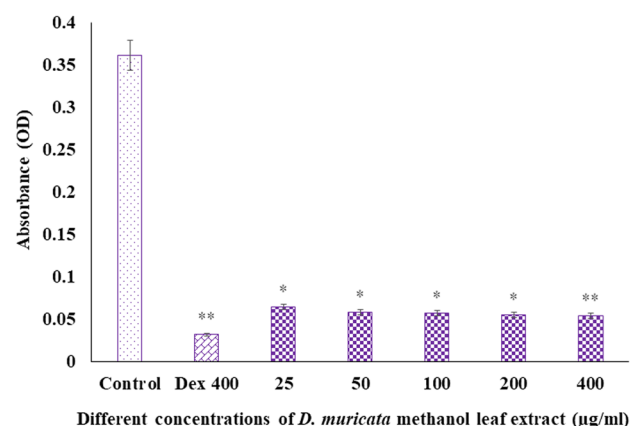


**Fig. 4** Anti-inflammatory activity of *D. muricata* leaf extract determined by its RBC membrane stabilization potential at different concentrations with dexamethasone (400 µg/ml) as a standard reference drug. Each data represent the mean ± SD of three determinants. The differences in the RBC membrane stabilization between control and treated cells were significant at \* $p < 0.05$  and \*\* $p < 0.01$

## Determination of cell viability using alamar blue and observation of cytomorphology

### Effects of 7-ketocholesterol on viability and cytomorphology of M2 phenotypic IC-21 macrophages

The cellular viability assay for M2 phenotypic IC-21 macrophages treated with 7KCh at five different concentrations (2, 4, 6, 8 and 10  $\mu\text{g/ml}$ ) assessed with incubation of 0.1% alamar blue revealed that the concentrations at 2, 4, 6 and 8  $\mu\text{g/ml}$  did not show any remarkable changes in the cell viability of IC-21 macrophages upon 24 h of incubation (Fig. 5A). A significant reduction in cell viability was observed at the highest tested concentration of 10  $\mu\text{g/ml}$  ( $*p < 0.05$ ). Supportive evidence was obtained from the morphological observation of the macrophages treated with 7KCh (Fig. 5B). Cells treated with 2, 4 and 6  $\mu\text{g/ml}$  concentrations of 7KCh (Fig. 5B b–d) were found to have normal morphology resembling the untreated control cells (Fig. 5B a), whereas, the cells treated with 8 and 10  $\mu\text{g/ml}$  concentrations showed cellular stress with round morphology and detached cellular appearance when observed

under an inverted phase-contrast microscope after 24 h of treatment (Fig. 5B e and f). It is evident from the results obtained from cell viability and morphological assessments of 7KCh that it put forth a dose-dependently decreased impact on macrophages.

### Effects of lipopolysaccharide on viability and cytomorphology of M2 phenotypic IC-21 macrophages

LPS at five different concentrations (25, 50, 100, 200 and 400 ng/ml) was studied for its effect on the alterations in cellular viability of M2 phenotypic IC-21 macrophages at 24 h. The results of cell viability assessed with alamar blue assay revealed that the macrophages did not show any remarkable change in the percentage of cell viability at lower tested concentrations (25–200 ng/ml; Fig. 6A), whereas, a significant reduction in the cell viability was detected at the maximum concentration tested (400 ng/ml) when compared to that of control cells (Fig. 6A;  $*p < 0.05$ ). Obtained viability data correlated with the morphological assessment where macrophages treated with lower concentrations (25–200 ng/ml; Fig. 6B b–e) were morphologically similar to that of control cells (Fig. 6B a). Distortion in the morphology was observed

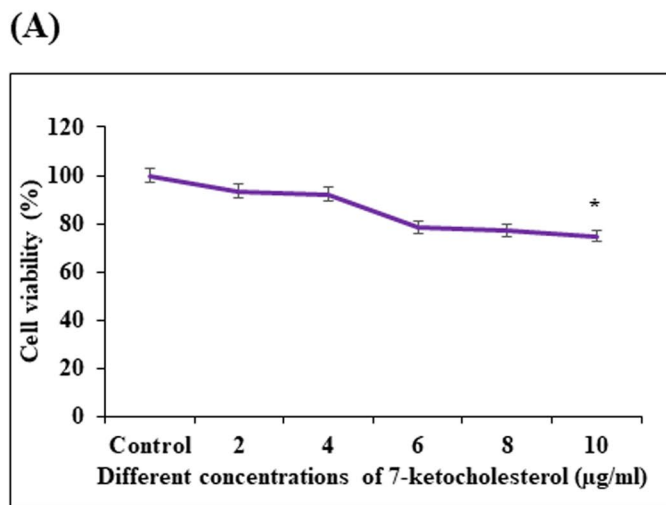
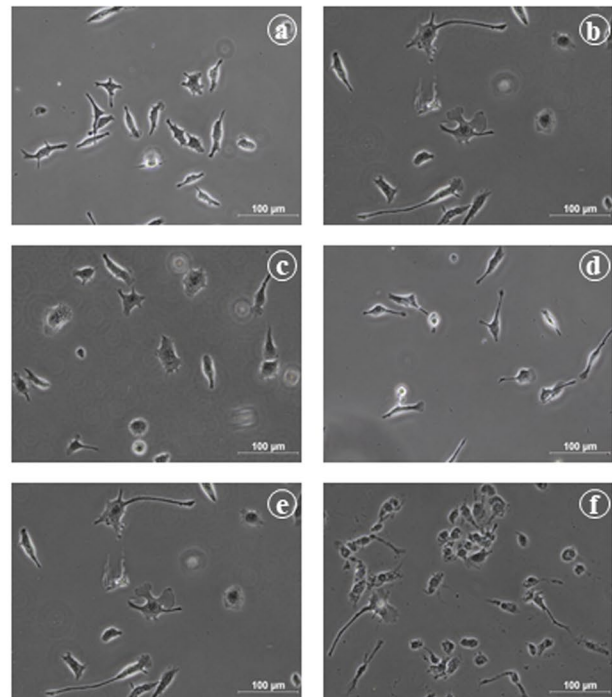


**Fig. 5** Effects of 7-ketocholesterol on viability and cytomorphology of M2 phenotypic IC-21 macrophages. **A** Percentage of cell viability of macrophages treated with different concentrations of 7-ketocholesterol (7KCh) for 24 h assessed by Alamar blue reagent. Each data represent the mean  $\pm$  SD of three determinants. The differences in the

(B)



cellular viability between control and treated cells were significant at  $*p < 0.05$ . **B** Cytomorphology of macrophages under control condition (a) and treatment with different concentrations of 7KCh (b 2  $\mu\text{g/ml}$ ; c 4  $\mu\text{g/ml}$ ; d 6  $\mu\text{g/ml}$ ; e 8  $\mu\text{g/ml}$  and f 10  $\mu\text{g/ml}$ )

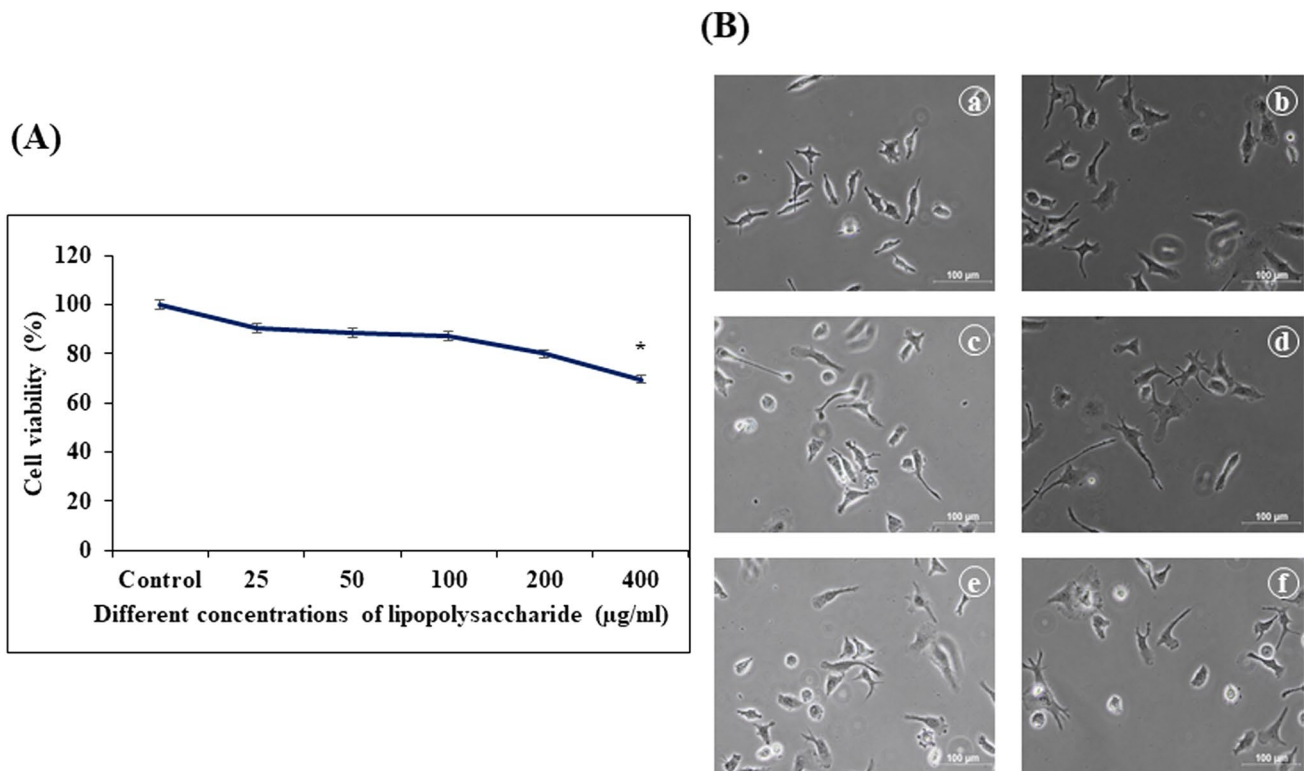


**Fig. 6** Effects of lipopolysaccharide on viability and cytomorphology of M2 phenotypic IC-21 macrophages. **A** Percentage of cell viability of macrophages treated with different concentrations of lipopolysaccharide (LPS) for 24 h assessed by alamar blue reagent. Each data represents the mean  $\pm$  SD of three determinants. The differences in

the cellular viability between control and treated cells were significant at  $*p < 0.05$ . **B** Cytomorphology of macrophages under control condition (a) and treatment with different concentrations of LPS (b 25 ng/ml; c 50 ng/ml; d 100 ng/ml; e 200 ng/ml and f 400 ng/ml)

at the maximum concentration tested (400 ng/ml; Fig. 6B f). The resulting data evidently displayed a dose-dependency of LPS for its effect on cell viability and morphological alteration of macrophages.

#### Effect of *Digera muricata* leaf extract on viability and cytomorphology of M2 phenotypic IC-21 macrophages

Cells treated with different concentrations of *D. muricata* leaf extract (25, 50, 100, 200, 400, 600, 800 and 1000 µg/ml) were assessed for the cellular viability of M2 phenotypic IC-21 macrophages with 0.1% alamar blue, and the results revealed that the extract at lower tested concentrations of 25–400 µg/ml showed no significant reduction in cell viability after 24 h of treatment, whereas there were significant reductions in the cell viability when treated with higher concentrations of 600–1000 µg/ml which were less than 80% (Fig. 7A;  $*p < 0.05$  and  $**p < 0.01$ ). Similar results were observed under an inverted phase-contrast microscope with viable and healthy macrophages similar to the control cells (Fig. 7B a) at lower concentrations (25–400 µg/ml; Fig. 7A b–f). Morphological alterations expressing cellular membrane distortions with reduced

viable cells were displayed at maximum tested concentrations (600–1000 µg/ml; Fig. 7B g–i).

#### Nitric oxide generation upon 7KCh and LPS stimulation of M2 phenotypic IC-21 macrophage

The griess assay was employed to assess nitric oxide generation by indirect quantification with sodium nitrite as the standard. Cells treated with different concentrations of 7KCh (2–10 µg/ml) and LPS (25–400 ng/ml) at different time intervals (1–5 and 12 h) showed a dose-dependent increase in the nitric oxide generation when compared to that of control cells (Fig. 8A, B). Treatment with 8 µg/ml of 7KCh resulted in a high level of NO production at 5- and 24-h time intervals (Fig. 8A) and the cells treated with 200 ng/ml of LPS revealed significant production of NO at 5- and 24-h time intervals (Fig. 8B). Reduction in the level of NO by 7KCh and LPS at their highest tested concentrations (10 µg/ml and 400 ng/ml, respectively) may potentially be incurred by their reduced viability effect. From the overall observation of griess assay, one significant concentration for 7KCh (8 µg/ml) and LPS (200 ng/ml) was selected and used for further experimental studies.

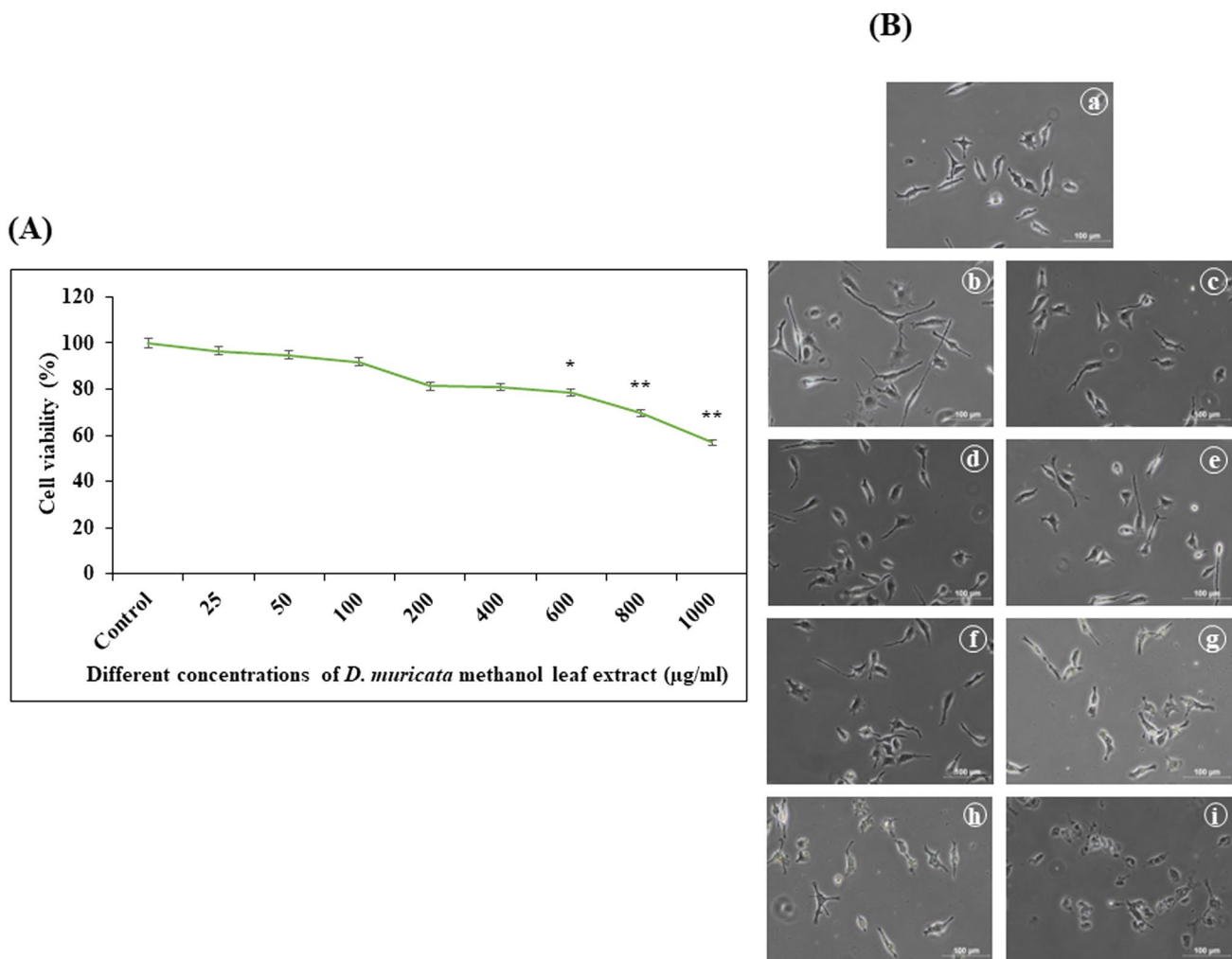


**Fig. 7** Effect of *Digeria muricata* leaf extract on viability and cytomorphology of M2 phenotypic IC-21 macrophages. **A** Percentage of cell viability of macrophages treated with different *D. muricata* leaf extract concentrations for 24 h assessed by alamar blue reagent. Each data represents the mean  $\pm$  SD of three determinants. The differences in the cellular viability between control and treated cells

were significant at  $*p < 0.05$  and  $**p < 0.01$ . **B** Cytomorphology of macrophages under control condition (a) and treatment with different concentrations of *D. muricata* leaf extract (b 25 µg/ml; c 50 µg/ml; d 100 µg/ml; e 200 µg/ml; f 400 µg/ml; g 600 µg/ml; h 800 µg/ml and i 1000 µg/ml)

### Impact of *D. muricata* leaf extract on nitric oxide generation stimulated by 7KCh and LPS

Control macrophages were found to release a very minimal NO (group I), but treating them with 7KCh (8 µg/ml) alone for 24 h resulted in an elevated level of NO (Fig. 9; group II). Co-stimulation of macrophages with 7KCh and LPS (group III) revealed an amplified NO generation owing to their synergistic effect with significance at  $**p < 0.01$  level when compared to the control cells (group I). Hence, LPS was used as an immunostimulant for the following assays. Interestingly, group IV treated with different concentrations of *D. muricata* leaf extract (group IV; 25–400 µg/ml) was observed to show significant (Fig. 9;  $*p < 0.05$

and  $**p < 0.01$ ) suppression in the release of NO in a dose-dependent manner even at the lowest tested concentration (group IV 25) when compared to that of group III (Fig. 9). The maximum inhibition of NO production was found to be employed by the highest tested viable concentration of 400 µg/ml (group IV 400), and hence, this active concentration was utilized for further analyses.

### Effect of *D. muricata* extract on arginase enzyme activity

Urea concentration was found to be lower in 7KCh and 7KCh + LPS-induced macrophages compared to the control cells (Fig. 10; group II and IV). Interestingly, the arginase

**Fig. 8** Quantification of nitric oxide (NO) generation upon 7KCh and LPS stimulation of IC-21 macrophages following Griess assay upon treatment with **A** 7-ketocholesterol and **B** lipopolysaccharide at various concentrations and time intervals. Each data represents the mean  $\pm$  SD of three determinants. The difference in the nitric oxide production between control and treated cells was significant at  $*p < 0.05$  and  $**p < 0.01$

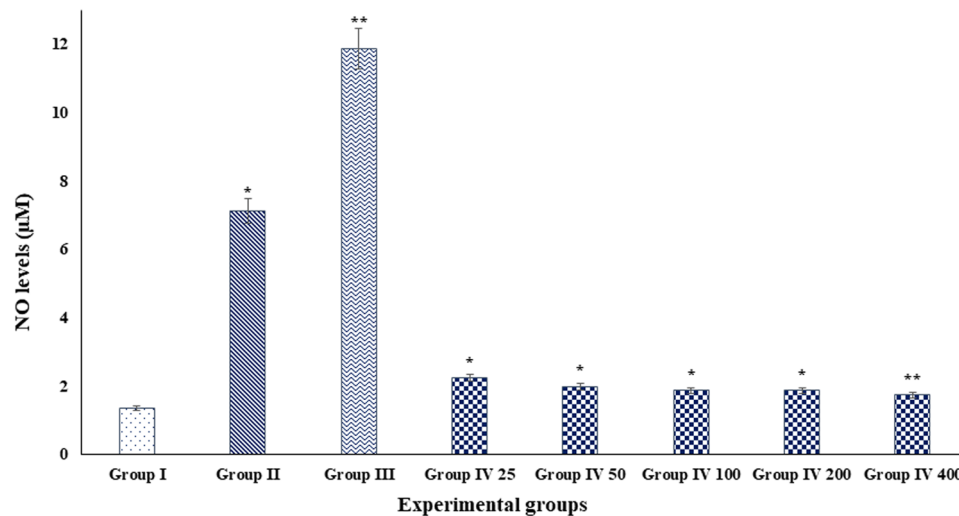
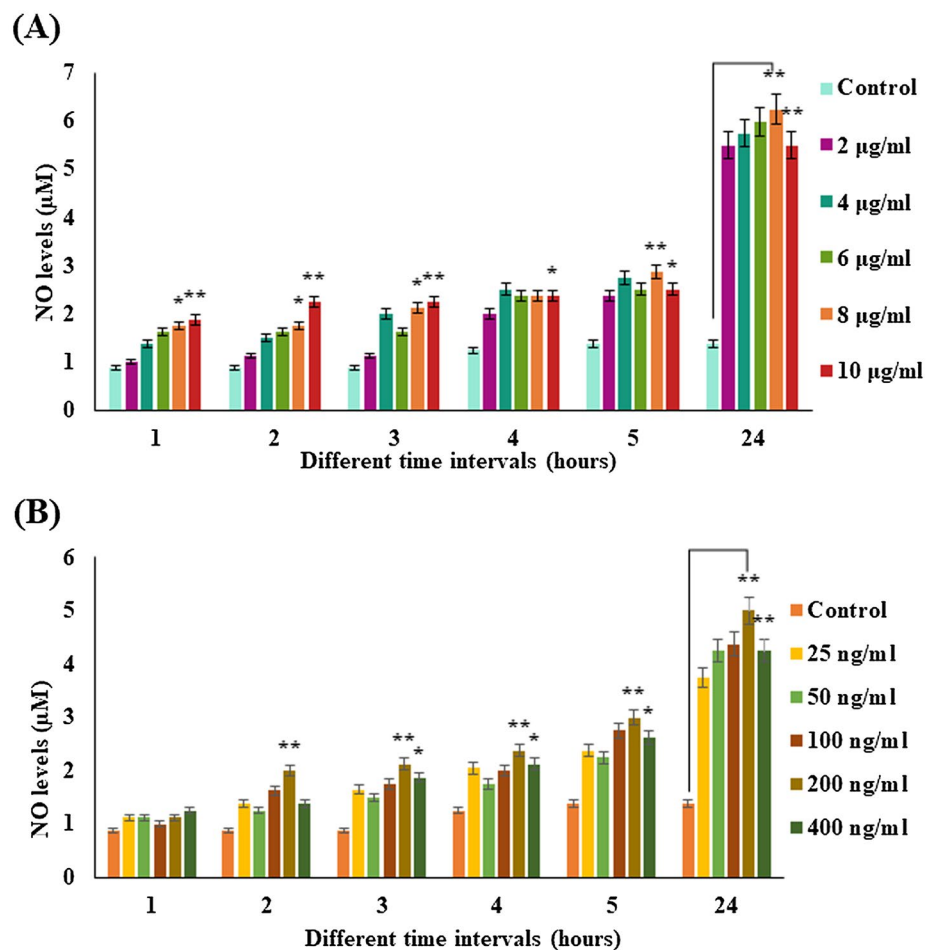


**Fig. 9** Quantification of nitric oxide (NO) generation by IC-21 macrophages following Griess assay upon treatment with different experimental groups (Group I—control cells; Group II—cells treated with 8 µg/ml of 7KCh; Group III—cells treated with 8 µg/ml of 7KCh and 200 ng/ml of LPS; Group IV 25–400—cells treated with 8 µg/ml of 7KCh, 200 ng/ml of LPS and co-treated with different concentra-

tions of *D. muricata* leaf extract) at 24-h time period. The effect of *D. muricata* leaf extract at different concentrations was estimated and compared with group III (7KCh+LPS) for significance in reduction. Each data represents the mean  $\pm$  SD of three determinants. The difference in the nitric oxide production between groups I and II–III and groups III and IV were significant at  $*p < 0.05$  and  $**p < 0.01$

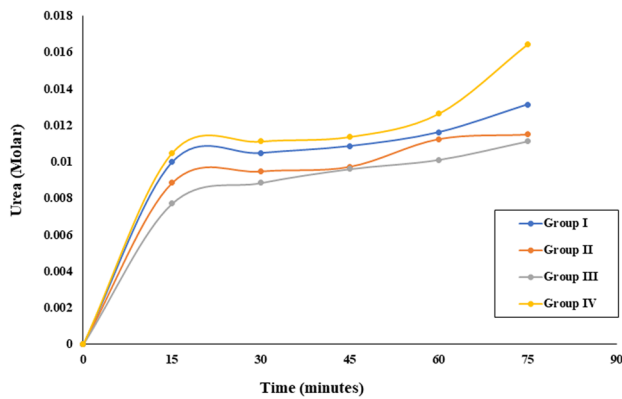


**Fig. 10** Effect of *D. muricata* leaf extract on arginase enzyme activity of M2 phenotypic IC-21 macrophages. Each data represents the mean  $\pm$  SD of three determinants

activity was found to be significantly higher in *D. muricata*-treated cells compared to the remaining experimental groups (Fig. 10; group IV). The enzyme activity increased with time and was highest at 75 min of incubation with the substrate.

### Effect of *D. muricata* extract on pinocytotic activity by neutral red uptake method

The pinocytotic activity assay of IC-21 macrophages by using the neutral red uptake method revealed higher endocytic activity under control conditions (Fig. 11; group I), whereas, macrophages treated with 7KCh (group II) showed

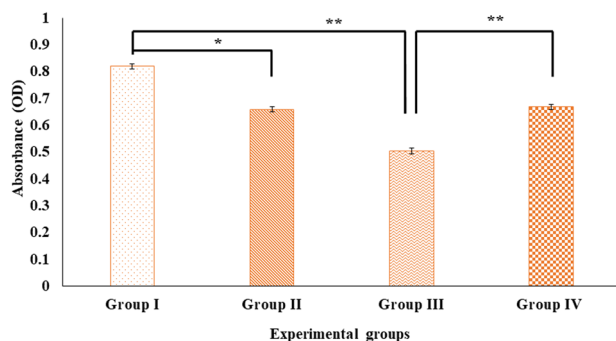


**Fig. 11** Pinocytotic activity of IC-21 macrophages was determined by neutral red dye uptake upon treatment with different experimental groups (Group I—control cells; Group II—cells treated with 8  $\mu$ g/ml of 7KCh; Group III—cells treated with 8  $\mu$ g/ml of 7KCh and 200 ng/ml of LPS; Group IV 25–400—cells treated with 8  $\mu$ g/ml of 7KCh, 200 ng/ml of LPS and co-treated with 400  $\mu$ g/ml of *D. muricata* leaf extract). Significant differences in the amount of neutral red uptake following 24 h of treatment suggest a potential difference in the pinocytotic capacity of macrophages. Each data represents the mean  $\pm$  SD of three determinants. The difference in the pinocytotic activity between groups I and II–III and groups III and IV were significant at  $*p < 0.05$  and  $**p < 0.01$

comparatively decreased pinocytotic activity. Macrophages upon treatment with 7KCh + LPS (group III) exhibited significantly ( $**p < 0.01$ ) lesser uptake of neutral red when compared to the control (group I). Interestingly, *D. muricata* extract (group IV; 400  $\mu$ g/ml)-treated macrophages showed a significantly increased pinocytosis by higher uptake of neutral red when compared to group III macrophages (Fig. 11).

### Effect of *D. muricata* extract on the accumulation of lipids in M2 phenotypic IC-21 macrophages

Foam cell formation of macrophages by lipid uptake was evaluated with Oil red O which is a lysochrome diazo dye used for the staining and quantification of intracellular lipid accumulation (Xu et al. 2010). Estimation of accumulated lipid level in experimented macrophages using oil red O staining revealed a significantly higher accumulation of lipids with increased absorbance in groups II and III upon exposure to 7KCh and 7KCh + LPS, respectively, when compared to the control (Fig. 12A; group I). In contrast, cells co-treated with leaf extract of *D. muricata* showed a significant reduction at  $**p < 0.01$  level (group IV), thereby showing a decrease in the amount of lipid accumulated which was similar to that of control cells (Fig. 12A; group I). We presumed that LPS aided in TLR4 receptor activation in macrophages which efficiently involved them in the uptake of administered 7KCh.

### Effect of *D. muricata* leaf extract on lipid peroxidation using thiobarbituric acid (TBA)

Our results obtained from the assessment of lipid peroxidation using thiobarbituric acid (TBA) showed that the 7KCh alone (Fig. 12B; group II) was able to induce the peroxidation of intracellular lipid which was comparatively greater than the control cells (group I). The synergistic effect of 7KCh and LPS (group III) was able to significantly increase at  $*p < 0.05$  level of lipid peroxidation when compared to groups I and II treated macrophages. This increased peroxidation was counteracted by co-treatment with *D. muricata* extract (Fig. 12B; group IV) which resulted in a significantly reduced ( $**p < 0.01$ ) level which was almost similar to that of control cells (group I).

### *D. muricata* leaf extract on ROS generation in M2 phenotypic IC-21 macrophages

DCFH-DA was used to detect ROS levels in the experimented cells qualitatively as well as quantitatively. Qualitative observation under a fluorescent microscope with

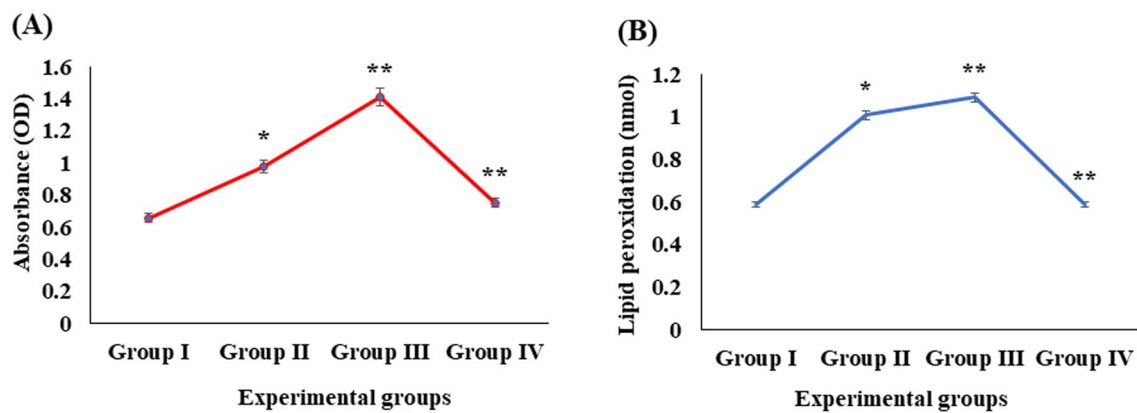


**Fig. 12** **A** 7-ketocholesterol uptake by IC-21 macrophages was quantified using lipid accumulation assay with oil red O staining in experimental groups (Group I—control cells; Group II—cells treated with 8  $\mu\text{g/ml}$  of 7KCh; Group III—cells treated with 8  $\mu\text{g/ml}$  of 7KCh and 200 ng/ml of LPS; Group IV 25–400—cells treated with 8  $\mu\text{g/ml}$  of 7KCh, 200 ng/ml of LPS and co-treated with 400  $\mu\text{g/ml}$  of *D. muricata* leaf extract) after 24 h. Each data represents the mean  $\pm$  SD of three determinants. The difference in the lipid accumulation levels between groups I and II–III and groups III and IV were significant at  $*p < 0.05$  and  $**p < 0.01$ . **B** Total lipid peroxidation level measure-

ment of thiobarbituric acid reactive substances (TBARS) in IC-21 macrophages following treatment with different experimental groups (Group I—control cells; Group II—cells treated with 8  $\mu\text{g/ml}$  of 7KCh; Group III—cells treated with 8  $\mu\text{g/ml}$  of 7KCh and 200 ng/ml of LPS; Group IV 25–400—cells treated with 8  $\mu\text{g/ml}$  of 7KCh, 200 ng/ml of LPS and co-treated with 400  $\mu\text{g/ml}$  of *D. muricata* leaf extract). Each data represents the mean  $\pm$  SD of three determinants. The difference in the lipid peroxidation levels between groups I and II–III and groups III and IV were significant at  $*p < 0.05$  and  $**p < 0.01$

ROS-specific DCFH-DA dye showed that the ROS production level in group II (7KCh) cells was increased than in the control cells (Fig. 13A; group I). When an LPS concentration of 400 ng/ml was treated along with 8  $\mu\text{g/ml}$  of 7KCh (group III), the ROS production was observed to be significantly higher than 7KCh alone treated and control macrophages (group I). Contrastingly, cells co-treated with the extract of *D. muricata* (group IV) showed significantly reduced ROS generation when compared to that of control cells (Fig. 12A; group I). Similar results were obtained during the quantification of fluorescence in experimental groups (Fig. 13B).

### ***D. muricata* extract on intracellular superoxide anion ( $\text{O}_2^-$ ) generation in M2 phenotypic IC-21 macrophages**

$\text{O}_2^-$  produced by some of the phagocytic cells under in vitro conditions is insufficient for extracellular detection using a microscopic NBT assay. Hence, a colorimetric NBT assay was performed for the detection of the superoxide anion in IC-21 macrophages. The results demonstrate that the cells treated with 7KCh (group II) and 7KCh + LPS (Fig. 14; group III) showed higher superoxide anions generation (OD = 0.895 and 0.1245, respectively) when compared to the control condition (group I). Strikingly, group IV upon co-treatment with extract of *D. muricata* exhibited a remarkably lower level of superoxide anions generation (OD = 0.75), similar to the control cells (Fig. 14; group I).

### **Influence of *D. muricata* extract on mitochondrial membrane potential**

Upon observing the experimented macrophages, we noted decreased fluorescent staining of mitochondrial with Rho123 in 7KCh as well as 7KCh + LPS-induced macrophages (Fig. 15; groups II and III) when compared to the control group (I). Interestingly, macrophages co-treated with *D. muricata* leaf extract (group IV) showed increased mitochondrial fluorescent emission which resembled the control (Fig. 15; group I). DAPI being a nucleic acid dye stained the nucleus of cells of all the experimental groups uniformly. This heterogeneity in fluorescent staining is attributed to the regulation of mitochondrial membrane potential by *D. muricata*.

### **Maintenance of cellular membrane integrity by *D. muricata* extract**

In order to observe the membrane integrity-associated well-being of macrophages, experimented macrophages were stained with nucleus-specific stains namely, acridine orange and ethidium bromide. The proportion of live and apoptotic cells was observed after 24 h of experimentation in different groups. Acridine orange is a permeable dye that emitted green fluorescence upon binding with the DNA of live cells, whereas ethidium bromide could enter a cell only upon membrane damage and it was



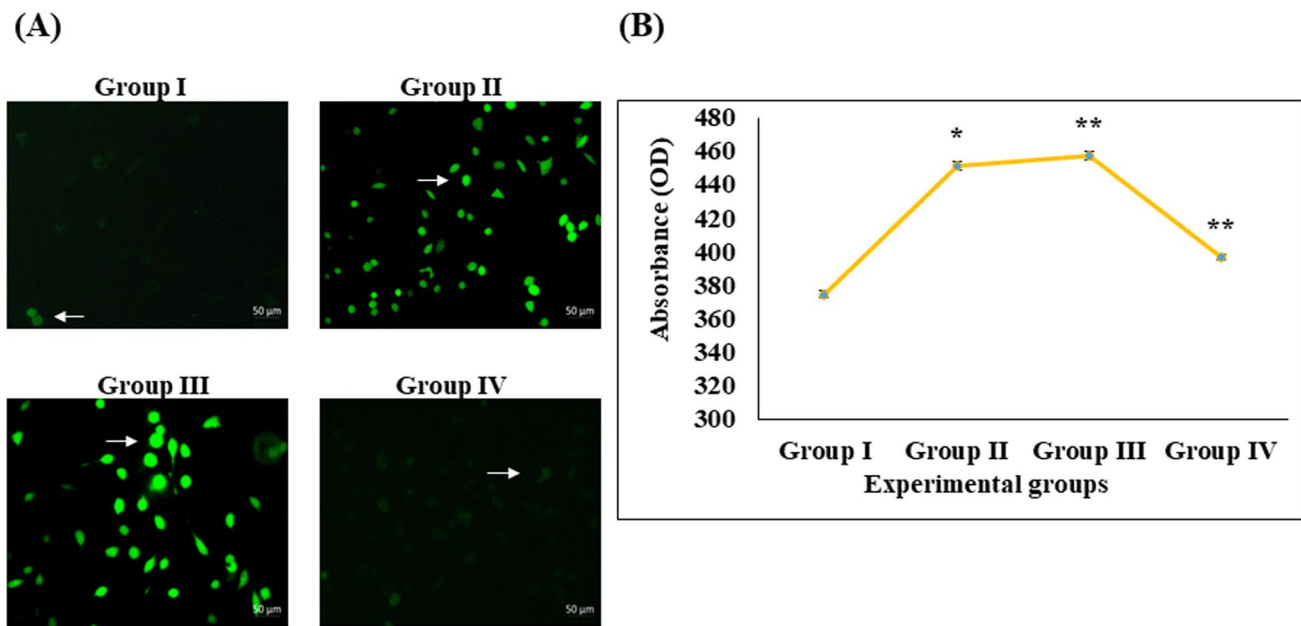


**Fig. 13** Quantitative and qualitative detection of ROS generation by DCFH-DA in M2 phenotypic IC-21 macrophages. **A** ROS level observed under a fluorescent microscope (→ in the figures denote the level of ROS generated inside the macrophages). **B** Estimation of ROS level produced by different experimental groups (Group I—control cells; Group II—cells treated with 8  $\mu\text{g/ml}$  of 7KCh; Group III—cells treated with 8  $\mu\text{g/ml}$  of 7KCh and 200  $\text{ng/ml}$  of LPS; Group IV

25–400—cells treated with 8  $\mu\text{g/ml}$  of 7KCh, 200  $\text{ng/ml}$  of LPS and co-treated with 400  $\mu\text{g/ml}$  of *D. muricata* leaf extract) after treatment for 24 h. The fluorescent absorbance (OD) was measured with a spectrofluorometer at an excitation of 485 nm and an emission of 530 nm. Each data represents the mean  $\pm$  SD of three determinants. The difference in the ROS levels between groups I and II–III and groups III and IV were significant at  $*p < 0.05$  and  $**p < 0.01$

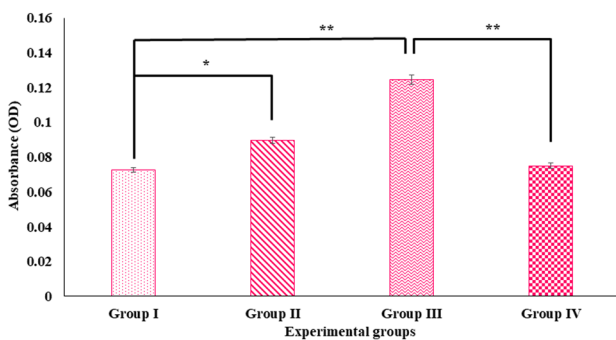


**Fig. 14** Level of superoxide generation estimated using NBT quantification assay in M2 phenotypic IC-21 macrophages (Group I—control cells; Group II—cells treated with 8  $\mu\text{g/ml}$  of 7KCh; Group III—cells treated with 8  $\mu\text{g/ml}$  of 7KCh and 200  $\text{ng/ml}$  of LPS; Group IV 25–400—cells treated with 8  $\mu\text{g/ml}$  of 7KCh, 200  $\text{ng/ml}$  of LPS and co-treated with 400  $\mu\text{g/ml}$  of *D. muricata* leaf extract) after experimentation for 24 h. The levels are expressed as absorbance (OD). Each data represents the mean  $\pm$  SD of three determinants. The difference in the superoxide anion generation between groups I and II–III and groups III and IV was significant at  $*p < 0.05$  and  $**p < 0.01$

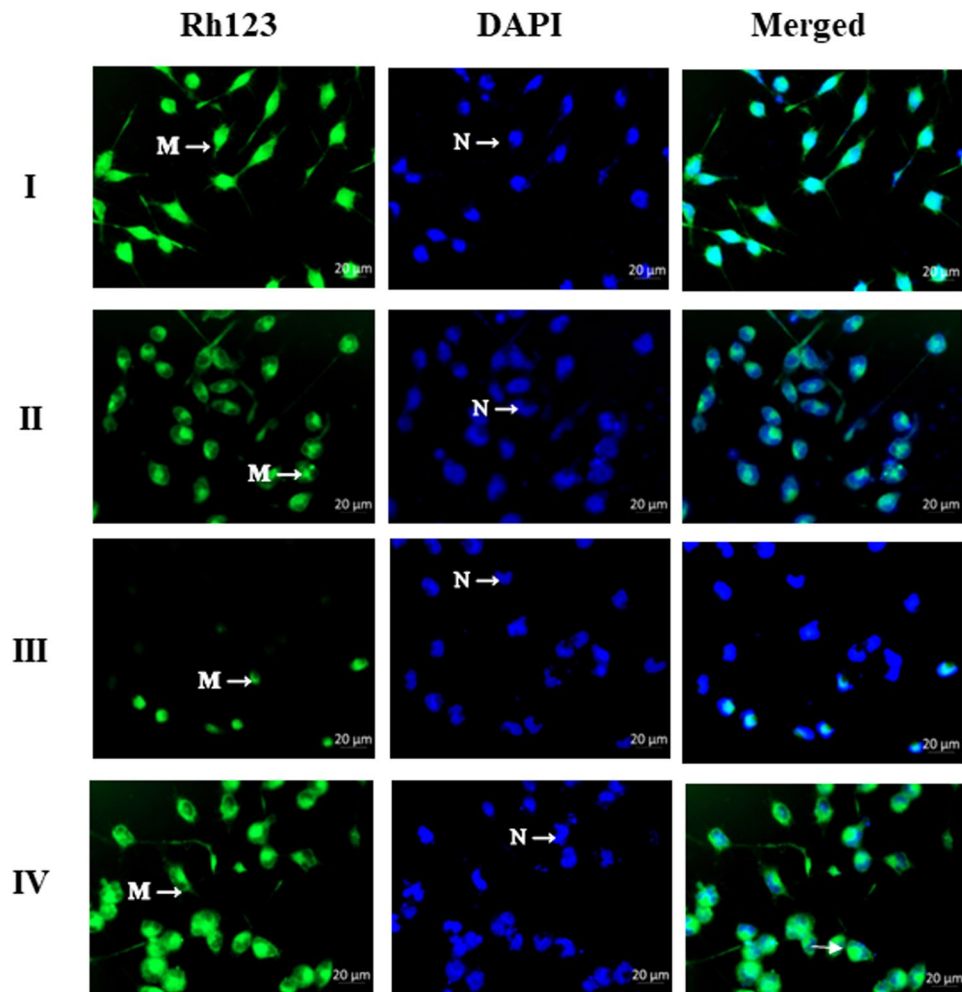
used to identify unhealthy cells undergoing early and late apoptosis. Cells under early apoptosis exhibited bright yellow-green coloured nuclei due to chromosome condensation and late apoptotic cells were stained red. Our

results indicated that the control group (Fig. 16; group I) was composed of live cells with no cells undergoing apoptosis. Induction with 7KCh (group II) results in early and late apoptosis of macrophages and the maximum level of apoptosis with the highest late apoptotic cells was evidently observed in 7KCh + LPS-induced cells (group III) compared to the control (group I). The effect of 7KCh and LPS on damaging the membrane integrity was effectively prevented upon co-treatment with *D. muricata* extract (Fig. 16; group IV) which showed the highest number of live cells with greatly reduced cells undergoing apoptosis almost similar to control cells (group I).

### Effect of *D. muricata* extract on mineralization of calcium in M2 phenotypic IC-21 macrophages

Intracellular calcium deposition was evaluated in experimental macrophages using an acid extraction method for quantification. Upon staining macrophages with ARS, mineralization of calcium was evident upon visualization. When the extracted stain was quantified colorimetrically, we observed that the groups (II and III) treated with 7KCh and 7KCh + LPS resulted in high calcium deposition with OD values of 0.057 and 0.061, respectively (Fig. 17). As anticipated, macrophages upon

**Fig. 15** Fluorescent imaging for mitochondrial membrane potential analysis of experimented IC-21 macrophages using rhodamine 123 (Rh123) and 4',6-diamidino-2-phenylindole (DAPI). Images expose the level of active mitochondria in live cells upon treatment with different experimental groups after 24 h (Group I—control cells; Group II—cells treated with 8  $\mu\text{g}/\text{ml}$  of 7KCh; Group III—cells treated with 8  $\mu\text{g}/\text{ml}$  of 7KCh and 200 ng/ml of LPS; Group IV 25–400—cells treated with 8  $\mu\text{g}/\text{ml}$  of 7KCh, 200 ng/ml of LPS and co-treated with 400  $\mu\text{g}/\text{ml}$  of *D. muricata* leaf extract). DAPI was used as a counter stain for the nucleus. Macrophages were observed under a confocal fluorescent microscope and the indications in the images are as follows: M  $\rightarrow$  active mitochondria and N  $\rightarrow$  nucleus



co-treatment with *D. muricata* extract expressed significantly reduced (group IV) calcium deposits with lower absorbance of OD value of 0.047 closely resembling the control group I (Fig. 17).

### Effect of *D. muricata* extract on expressions of inflammatory genes produced upon 7KCh and LPS induction

#### Pro-atherogenic enzymes (iNOS, COX-2 and MMP-9)

Inflammation is generally orchestrated by enzymes such as iNOS, COX-2 and MMP-9 produced by macrophages upon pro-inflammatory stimulation. Our expression analysis revealed that these genes of pro-atherogenic enzymes were significantly upregulated in 7KCh-treated cells and 7KCh+LPS-treated cells (group II and III, respectively) when compared with control cells (group I). On the contrary, their levels were remarkably downregulated upon co-treatment

with *D. muricata* leaf extract (group IV) which was closely similar to that of the control cells (Fig. 18; group I).

#### Pro-atherogenic interleukins (IL-6 and IL-1 $\beta$ )

Interleukins are inflammatory cytokines produced by macrophages among which IL-6 and IL-1 $\beta$  are pro-atherogenic in nature. Analysis of the genes responsible for these interleukin productions showed that they were highly elevated in groups II and III treated with 7KCh and 7KCh+LPS, respectively, than in the control group I. In contrast, when they are co-treated with *D. muricata* leaf extract (group IV) their levels are significantly reduced closely resembling the control cells (Fig. 18; group I).

#### Pro-atherogenic scavenging receptors (CD36 and CD163)

Scavenging receptors CD36 and CD163 are pro-atherogenic markers highly expressed on the surface of pro-inflammatory

**Fig. 16** Membrane integrity analysis of experimented IC-21 macrophages visualized under a confocal fluorescent microscope using acridine orange (AO) and ethidium bromide (EB) nuclear stains. Images expose the level of membrane integrity in cells upon treatment with different experimental groups after 24 h (Group I—control cells; Group II—cells treated with 8  $\mu\text{g}/\text{ml}$  of 7KCh; Group III—cells treated with 8  $\mu\text{g}/\text{ml}$  of 7KCh and 200 ng/ml of LPS; Group IV 25–400—cells treated with 8  $\mu\text{g}/\text{ml}$  of 7KCh, 200 ng/ml of LPS and co-treated with 400  $\mu\text{g}/\text{ml}$  of *D. muricata* leaf extract). Macrophages were observed and the indications in the images are as follows: L  $\rightarrow$  live cells; EA  $\rightarrow$  early apoptotic cells and LA  $\rightarrow$  late apoptotic cells

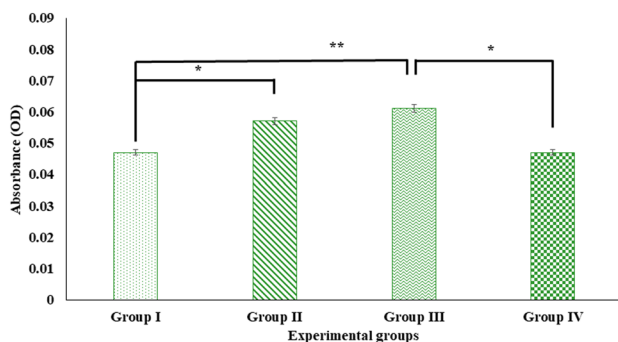
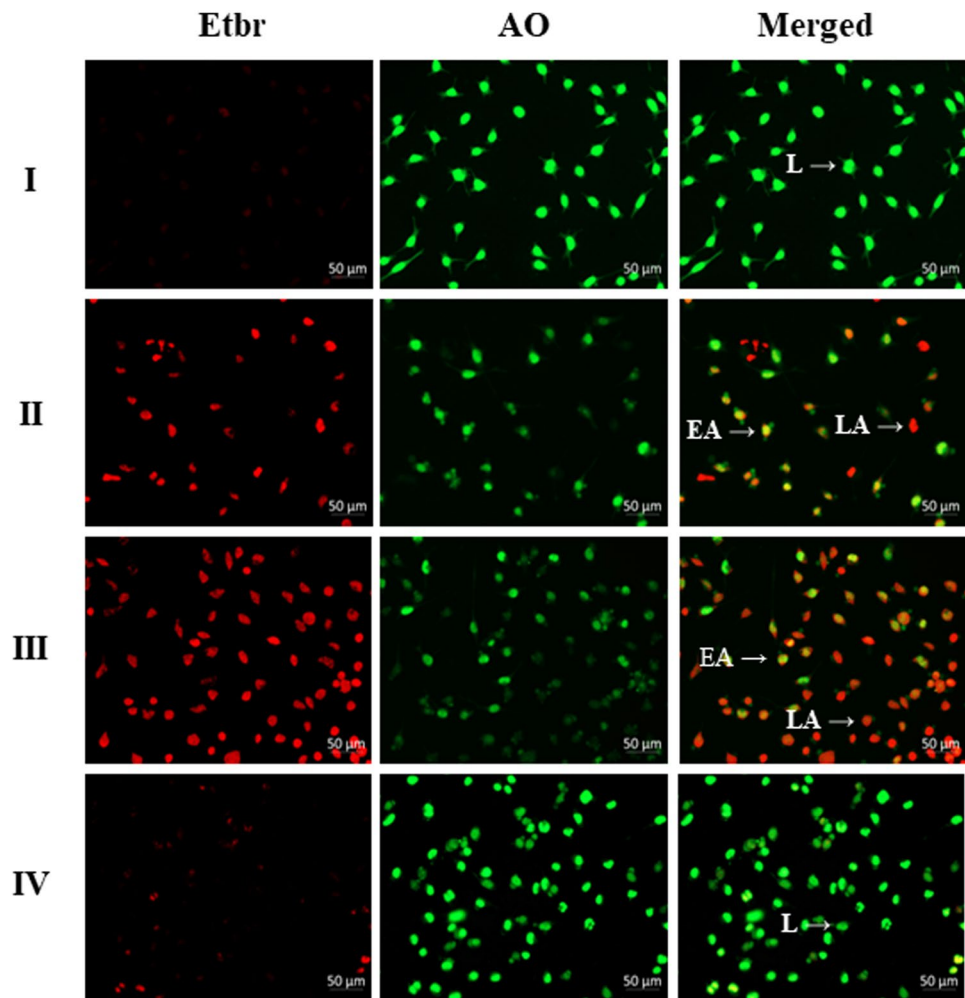


**Fig. 17** Quantitative analysis of intracellular calcium deposition in cultured M2 phenotypic IC-21 macrophages using alizarin red S staining. Data represents the level of calcium deposits in each of the experimental groups after 24 h of treatment (Group I—control cells; Group II—cells treated with 8  $\mu\text{g}/\text{ml}$  of 7KCh; Group III—cells treated with 8  $\mu\text{g}/\text{ml}$  of 7KCh and 200 ng/ml of LPS; Group IV 25–400—cells treated with 8  $\mu\text{g}/\text{ml}$  of 7KCh, 200 ng/ml of LPS and co-treated with 400  $\mu\text{g}/\text{ml}$  of *D. muricata* leaf extract). Each data represents the mean  $\pm$  SD of three determinants. The difference in the calcium deposition between groups I and II–III and groups III and IV were significant at  $*p < 0.05$  and  $**p < 0.01$

macrophages. We assessed the expression level of these receptor genes under experimental conditions. Our results illustrate that treatment of macrophages with 7KCh and 7KCh + LPS (groups II & III) significantly upregulated their levels compared to the control group, whereas, their levels were notably decreased upon co-treatment with *D. muricata* leaf extract (group IV) and closely resembled the control cells (Fig. 18; group I).

#### Anti-atherogenic surface receptors (MRC1 and PPAR $\gamma$ )

Along with pro-atherogenic inflammatory markers, we also analysed for the expression of anti-atherogenic markers namely MRC1 and PPAR $\gamma$  which are beneficial. MRC1 and PPAR $\gamma$  involve in tissue healing and remodelling for anti-inflammation. Our results on gene expression analyses of these beneficial macrophage markers show that their expression levels were lower in groups treated with 7KCh and 7KCh + LPS (groups II and III) than in the control group. Interestingly, when macrophages were co-treated with *D.*

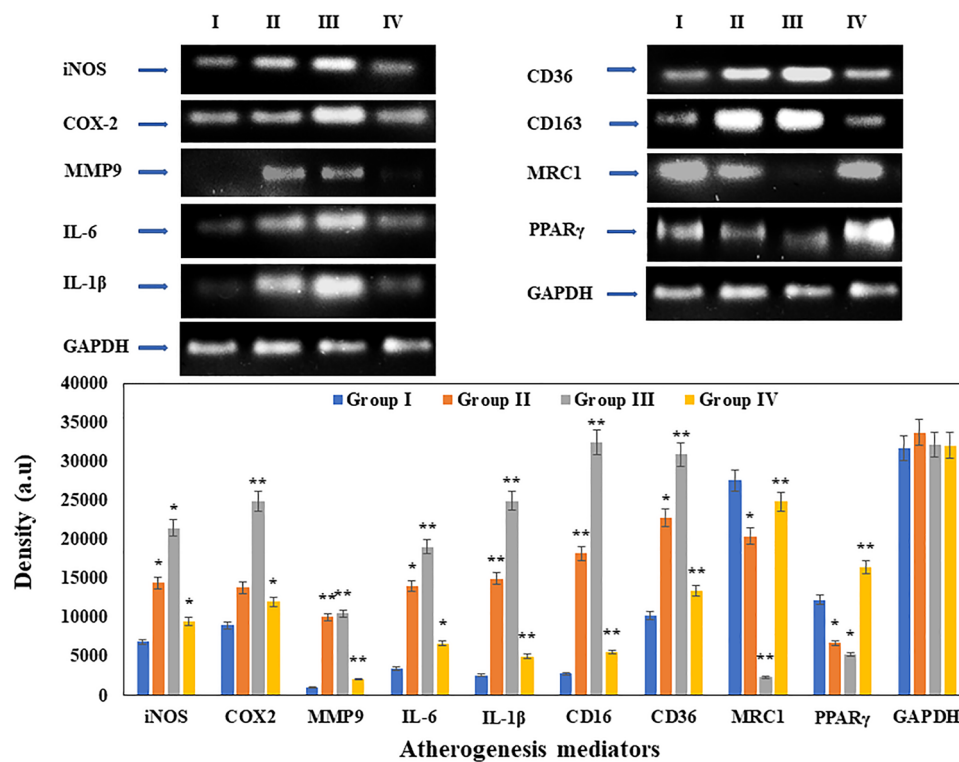


**Fig. 18** Gene expression of pro-atherogenic enzymes (iNOS, COX-2 and MMP-9), interleukins (IL-6 and IL-1 $\beta$ ), pro-atherogenic scavenging receptors (CD163 and CD36) and anti-atherogenic surface receptors (MRC1 and PPAR $\gamma$ ) which are specific for M1 and M2 phenotypic macrophages were analysed. Pro-atherogenic mediators were found to be upregulated, whereas anti-atherogenic mediators were downregulated in the 7KCh along and 7KCh+LPS treated cells (Groups II and III) compared to the control condition (Group I). From

the gel electrophoresis results, co-treatment with *D. muricata* leaf extract (Group IV) has evidently modulated the expression of macrophage mediators. Densitometric values of the obtained bands were plotted in graphs for comparison. Each data represents the mean  $\pm$  SD of three determinants. The difference in the gene expression levels between groups I and II–III and groups III and IV were significant at  $*p < 0.05$  and  $**p < 0.01$

*muricata* leaf extract (group IV) they expressed a higher level of surface receptors very much resembling control cells (Fig. 18; group 1).

### Effect of *D. muricata* leaf extract on expressions of TGF $\beta$ 1

Results obtained from the ELISA technique showed lower levels of TGF $\beta$ 1 in the groups treated with 7KCh and 7KCh+LPS (groups II and III) compared to the control group (Fig. 19). The concentration of TGF $\beta$ 1 was significantly higher in the supernatant obtained from the group co-treated with *D. muricata* leaf extract ( $2.8025 \pm 0.07$  ng/ml; group IV) than that of the remaining experimental groups.

### Protein expression of NF- $\kappa$ B and iNOS

Immunocytochemistry analysis showed that the cells treated with 7KCh and 7KCh+LPS (groups II and III) expressed higher expression of NF- $\kappa$ B p65 in the nuclear region compared to the control group. The co-treatment of

macrophages with *D. muricata* leaf extract (Fig. 20; group IV) down-regulated the expression of NF- $\kappa$ B p65 and it was similar to the control cells. Similar results were observed

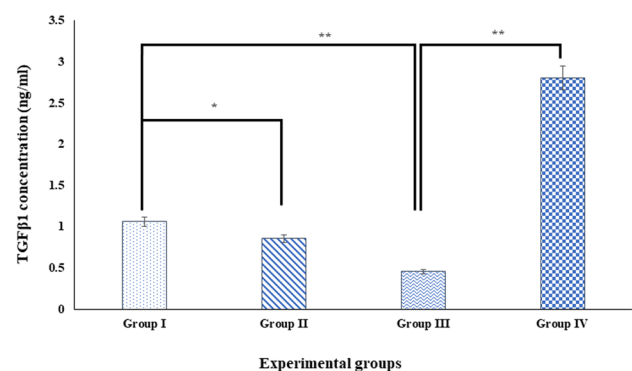


**Fig. 19** Effect of *D. muricata* leaf extract on the TGF $\beta$ 1 cytokine expression in M2 phenotypic IC-21 macrophages. Each data represents the mean  $\pm$  SD of three determinants. The difference in the TGF $\beta$ 1 cytokine level between groups I and II–III and groups III and IV were significant at  $*p < 0.05$  and  $**p < 0.01$

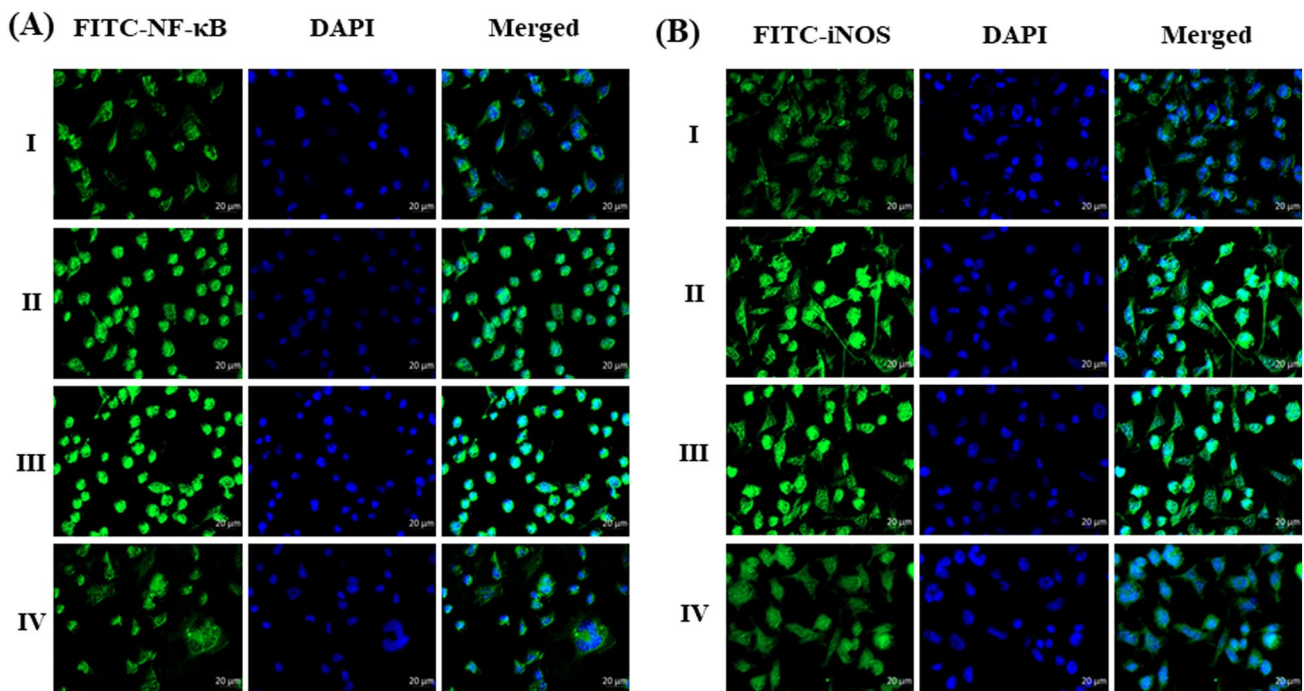


**Fig. 20** Effect of *D. muricata* leaf extract on protein expression of **A** nuclear transcription factor NF- $\kappa$ B and **B** pro-inflammatory mediator iNOS in M2 phenotypic IC-21 macrophages when induced with 7KCh and LPS

upon observing the expression of iNOS in the experimented cells which implied that treatment of *D. muricata* was significantly able to reduce NF- $\kappa$ B p65 and iNOS expression levels.

## Discussion

Medicinal plants have the potential to prevent and reduce atherosclerotic manifestations through their pleiotropic anti-inflammatory, anti-oxidant, anti-lipidemic and anti-thrombotic effects exhibited by their phytochemicals (Kirichenko et al. 2020). In this context, this study aimed to elucidate the anti-atherogenic activity of a traditionally consumed medicinal plant, *D. muricata* which is locally being used for treating multiple disorders associated with inflammation (Khan and Younus 2011). The presence of all the tested phytochemicals observed in the methanol extract was validated by the previous studies which stated the presence of such phytochemicals in the extract of *D. muricata* (Mathad and Mety 2010; Usmani et al. 2013). Ramalashmi (2019) reported the absence of saponins and steroids in the methanol leaf extract of *D. muricata* which is contradictory and requires further validation. In general, bioactive phytochemical constituents including polyphenols, flavonoids, steroids, and vitamins of medicinal plants like *Allium cepa* (onion), *Allium sativum* (garlic), *Ocimum sanctum* (holy basil), etc. have been proven to combat several diseases (Vasanthi et al.

2012). These phytochemicals have been suggested to be the prime responsible compounds with beneficial effects on human health, especially for cardioprotection (Liu 2003).

Phytochemical profiling with TLC and GCMS denoted the presence of various phytochemicals in the leaf extract of *D. muricata* and their retention factors of the compounds indicate an idea of their polarity. This will further help in the future for the selection of suitable solvent systems for the separation and isolation of a bioactive compound using column chromatography. Similar TLC profiling of aqueous leaf extract of *D. muricata* was separated by Mubark and Ahmed (2020). This qualitative analysis has been performed on several other medicinal plant extracts like *Cassia filiformis* (love-vine), *Daucus carota* (wild carrot), *Catharanthus roseus* (cape periwinkle), *Anredera cordifolia* (mignonette vine), etc. to identify and isolate phytochemicals for cardioprotection (Astuti et al. 2011; Sathiavelu and Arunachalam 2012; Kabesh et al. 2015; John et al. 2017). This analysis authenticates the visual confirmation of diverse phytochemicals present in the leaf extract making it suitable for further experimentation. Sitosterol is an important phytosterol that has been found to express protective activity against the foam cell formation of J774A.1 macrophage cell line and modulatory effect on oxidative stress induced by Ox-LDL (Vivancos and Moreno 2008; Rosenblat et al. 2013). This plant has already been reported to contain some of the pharmacologically significant phytochemicals like  $\alpha$  and  $\beta$ -spinasterol with nutritional interest that have been

extensively studied for their impact on mechanisms of cell responses, especially involving anti-oxidation and cellular signalling to prevent disease developments (Virgili and Marino 2008; Ghaffar et al. 2019).

In support of our results, the DPPH scavenging property of *D. muricata* extract was also reported previously with higher scavenging activity among other studied medicinal plants such as *Gomphrena serrata* (prostrate gomphrena), *Alternanthera paronychioides* (smooth joyweed) and *Celosia argentea* (prince of wales feathers) emphasizing its dynamic antioxidant activity (Shazia et al. 2013; Arulmuthi et al. 2017). The effective anti-oxidant activity of *D. muricata* leaf extract could be attributed to the presence of free radical scavenging constituents like hexadecanoic acid, sitosterol, phytol and tridecanoic acid (Henry et al. 2002; Santos and Salvadori 2013; Bharath and Perinbam 2021; Gupta et al. 2011). Similar analyses of plants such as *Hibiscus sabdariffa* (roselle) and *Solanum sisymbriifolium* (sticky nightshade) with higher free radical scavenging activities have been reported to suppress ROS production, LDL oxidation and Ox-LDL-mediated apoptosis in macrophages which are pro-inflammatory in action (Chang et al. 2006; More and Makola 2020). In this context, the anti-inflammatory property of this extract was tested further.

RBC membrane stabilization test remains to be one of the classical techniques to preliminarily evaluate the anti-inflammatory property of a drug (Sur et al. 2002). The cellular membrane integrity of immune cells like macrophages is greatly affected during oxidative stress and its protection is vital for its normal functioning (Coquette et al. 1986). Oxidized lipid products have been shown to exert cytotoxic effects on macrophages by disrupting their membrane homeostasis, causing destabilization of lysosomes and mitochondria, which is a crucial event in the macrophage foam cell necroptosis (Yuan et al. 2000). Hence, an anti-inflammatory drug with efficient cytoprotective activity is critical for maintaining macrophage integrity to prevent plaque progression during atherogenesis. In this study, the extract was able to prevent the hypotonicity-induced membrane instability of hRBC effectively even at the lowest concentration resembling the standard drug, thereby suggesting its protective effect in modulating inflammatory mediators. Surprisingly, the membrane stabilization activity of the extract was almost equal to the effect of dexamethasone even at the lowest concentration tested. This indicated the efficiency of the extract to exert a potential anti-inflammatory effect, thereby preventing macrophage polarization.

7KCh was found to be the most cytotoxic at higher concentrations to cultured cells upon internalization among the predominant oxysterols (Rodriguez et al. 2004). The proapoptotic feature of 7KCh was able to kindle the death of murine macrophages through caspases of the mitochondrial apoptotic pathway (Biasi et al. 2004). A dose-dependent

decrease in human macrophage THP-1 cells was reported upon treatment with 7KCh up to 25  $\mu\text{M}$  concentration similar to our results. This was found to be due to 7KCh's ability in arresting cell cycle progression preferably through oxidative stress of DNA (Palozza et al. 2010). In addition, the cellular apoptosis of murine macrophage cell line J774A.1 was exposed to be through the involvement of NF- $\kappa$ B activation by means of dose and time dependency (Huang et al. 2010). LPS has been extensively analysed for its induction of apoptosis through a spectrum of cytomorphological as well as biomolecular changes mediated by mitochondrial and nuclear damage (Forbes-Hernández and Giampieri 2014). Its effect on inducing inflammation and apoptosis is also applicable to macrophages by molecular mechanisms involving several signalling pathways in a dose-dependent fashion, thereby affecting their cell viability (Afrin et al. 2018). Activation of macrophages at a viable concentration was found to induce the production of inflammatory mediators, namely, NO and associated cytokines through its TLR4-mediated signalling (Padwad et al. 2006). LPS was assessed at very low concentrations in this study to avoid its dominance in inducing a synergistic activity on macrophages as it was used only for co-stimulation with 7KCh. *D. muricata* has been studied to expose concentration-dependent reduction in the viability of cells at higher concentrations (Deepthi et al. 2021). Hence, in this study, the viable concentrations were utilized for further analyses to maintain the viability of macrophages. The effect of *D. muricata* extract had not been assessed on macrophages so far; this is the first time it has been studied for its protective effect under in vitro conditions.

Nitric oxide is a reactive nitrogen species and cytotoxic effector synthesized by macrophages through iNOS towards its contribution to regulating inflammatory events (Boscá et al. 2005). Increased production of NO is known to mediate cytotoxicity and apoptosis of vascular cells during pro-atherogenesis as well as cause vasodilation resulting in inflammation and septic shock (Li and Horke 2014; Förstermann et al. 2017). It is a predominant marker of M1 phenotypic macrophages which synthesizes it through iNOS by regulating NF- $\kappa$ B signalling (Colin et al. 2014). 7KCh has been found to induce increased production of ROS/RNS in cells, especially macrophages that lead the cells towards apoptosis (Leonarduzzi et al. 2006). In addition, 7KCh has also been shown to support the polarization of macrophages towards the M1 phenotype by increasing its pro-inflammatory characteristic production of cytokines and chemokines, especially iNOS (Drvar et al. 2022). Elevated expression of inflammatory mediator iNOS in 7KCh-exposed macrophages is responsible for the higher production of NO, thereby modulating its phenotype (Calle et al. 2019; Duraisamy et al. 2023). These previous findings highly correlate with our results of increased NO production

upon 7KCh treatment with dose dependency. In our findings, we observed that even at very lesser concentrations, LPS could achieve overproduction of NO. Previous studies support this by demonstrating its efficiency in inducing NO production through iNOS expression in macrophages (Ghosh 1999; Ryu et al. 2003; Choe and Choi 2019; Moore et al. 2019). Thus, it was used in this study as a co-stimulant to achieve a rapid atherogenic environment under in vitro conditions. Plants with medicinal values possess natural antioxidant properties due to their varied phytochemicals which aid in ameliorating nitric oxide radicals that are destructive to tissues (Rasheed and Azeez 2019). The antioxidant property of *Digera muricata* was previously reported (Elgailani 2018; Mehwish and Islam 2019), and this may have possibly conferred its effect on significant reduction of NO production in macrophages in this study. Similarly, previous reports prove that extracts of *Populus maximowiczii*, *Gynura procumbens*, *Machilus thunbergii*, *Ranunculus sceleratus* *Artemisia iwayomogi* and *Populus davidiana* with antioxidant properties were shown to potentially inhibit NO in macrophages (Ryu et al. 2003; Ning et al. 2019; Marrelli et al. 2022). Reduction of M1 macrophage-synthesized nitric oxide by a plant molecule, protocatechuic acid (PCA) has been shown to attenuate atherogenesis by inhibiting M1 macrophage polarization (Liu et al. 2018). Similar attenuation of abnormal macrophage polarization was analysed through diverse methodologies further in this study.

Nitric oxide generation that is distinctive to M1 macrophages is indirectly proportional to M2 macrophage-specific arginase enzyme activity since they are involved in the metabolism of L-arginine (Yang and Ming 2014). Based on our results, it is evident not only that 7KCh and LPS were able to induce abnormal macrophage polarization through decreased arginase activity but also the effect of *D. muricata* in increasing the arginase activity that is highly necessary for macrophage in mediating anti-inflammation during atherogenesis (Fig. 9). Studies report evidence of 7KCh mediating the decrease in arginase expression, thereby influencing the polarization of macrophage towards the M1 phenotype (Drvar et al. 2022). Alcoholic extracts of herbal immunomodulators belonging to the *Echinacea* genus such as *E. angustifolia*, *E. pallida* and *E. purpurea* have been found to significantly increase arginase activity in stimulated RAW 264.7 macrophages (Zhai et al. 2009). In contrast, arginase enzyme activity was assessed as a major marker of M2 phenotype in macrophages and our results indicated that the effect of *D. muricata* in reducing the NO production was through the increased production of arginase (Fig. 10). These competing arginine metabolism pathways have been well-studied to influence macrophage polarization processes during atherosclerosis (Rath et al. 2014).

IC-21 macrophage is an M2 phenotype macrophage cell line with enhanced endocytic activity under normal

conditions. Cholesterol and its derivatives accumulate in macrophages and turn them into lipid-laden foam cells that contribute to atherosclerotic plaque development (Kruth 2011). 7KCh has been found to promote foam cell formation of macrophages that displayed pro-inflammatory characteristics with poor sterol efflux transport (Gelissen et al. 1996; Hayden et al. 2002). Intracellular accumulation of 7KCh has been found to modulate the endocytic responses of murine macrophages (Ravi et al. 2021). Our results clearly indicate the restoration of pinocytosis in macrophages which was impaired by 7KCh and LPS. This may possibly be due to the effect of *D. muricata* leaf extract in the prevention of lipid uptake and formation of foam cells or by enhancing the cholesterol efflux pathways which was analysed in further experiments (Li and Glass 2002).

Similar to our findings, recent studies show that upon accumulation of 7KCh in macrophages, atherosclerotic responses are produced that are responsible for disease progression (Biasi et al. 2004; Rao et al. 2014). Several plants like piper betel, pomegranate, *Castanea molissima* and their biomolecules such as polyphenols, sterols and stanols were claimed to prevent or inhibit the accumulation of lipids in macrophages as well as augment cholesterol efflux pathways (Ma et al. 2013a, b; Gylling et al. 2014; Zhao et al. 2016; Liu and Lu 2022). 7KCh-induced atherosclerotic side effects were found to be counteracted upon treatment with numerous natural compounds, especially medicinal plants (Brahmi et al. 2018, 2019). *D. muricata* is one among such medicinal plants which have shown promising results in our study by efficiently lowering the lipid accumulation in macrophages upon co-treatment (Fig. 12A; group IV), thereby proving its role in atheroprotection by preventing lipid uptake. The possible reason behind our results of *D. muricata* in preventing lipid uptake may be due to its potential anti-lipidemic activity or its regulation of lipid metabolism and efflux.

7KCh has been analysed previously for its lipid peroxidation activity through malondialdehyde formation (Monier et al. 2003). Similar evidence was obtained from our experiment when macrophages were treated with 7KCh (group II; Fig. 12B). Inhibition of lipid peroxidation with plant-based anti-oxidant supplementation has been found to prevent the formation of foam cells and atherogenesis (Kaplan et al. 2001). Since 7KCh and LPS increased the level of lipid peroxidation in macrophages, it made us curious to know whether this effect is induced by intracellular oxidative stress. Thus, we assessed the level of ROS and  $O_2^-$  in particular, under experimental conditions.

The generation of reactive oxygen species results in oxidative stress that leads to inflammation and causes atherosclerosis. According to Kattoor et al. (2017), reactive oxygen species (ROS) are a group of small reactive molecules that play vital roles in regulating cell functions and biological processes. Mitochondrial oxidative stress in atherosclerotic

macrophages produced upon LDL increase was found to amplify lesion formation (Wang et al. 2014). Oxysterols such as 7-ketocholesterol at 16  $\mu\text{M}$  concentration enhanced the production of reactive oxygen species (Palozza et al. 2010). Likewise, under our in vitro experiment, we assessed the level of ROS generation quantitatively as well as qualitatively using DCFH-DA dye under the influence of 7KCh, an ox-LDL with or without LPS as an immunostimulant and our results correlate with the previous studies as an increased ROS level was observed (Brahmi et al. 2018). This phenomenon was retained to normalcy upon co-treatment with *D. muricata* leaf extract with reduced ROS levels (Fig. 13A, B). Prior studies with this plant extract also support its antioxidant ability when administered with toxic substances like carbon tetrachloride ( $\text{CCl}_4$ ) (Khan et al. 2009; Muhammad et al. 2011).

Macrophages produce a burst of superoxide anion mediated by NADPH oxidase upon activation in atherogenesis (Cathcart 2004) and correspondingly in our study treatment of macrophages with 7KCh along with or without LPS (Fig. 14; groups II and III) drastically increased their levels. As superoxide anions contribute to the pathogenesis of inflammatory diseases including atherosclerosis, reducing it would be a better therapeutic strategy. Upon co-treatment with *D. muricata* methanol extract, the level of superoxide anion generation was found to be beneficially reduced (Fig. 14; group IV). Plant alkaloids such as berberine involve in inhibiting NADPH oxidase-mediated superoxide anion production in macrophages (Sarna et al. 2010). Several pharmacologically important plants namely *Cucumis melo* (Vouldoukis et al. 2004), *Rhus verniciflua* (Jung et al. 2006), *Limonium densiflorum* (de Medina et al. 2009), *Phyllanthus acidus* (Manikandan et al. 2017), *Smilax campestris* (Salaverry and Parrado 2020), etc., provided a free radical scavenging activity that possesses anti-oxidant functions similar to *D. muricata* in this study. Plants belonging to Amaranthaceae namely, *Amaranthus spinosus* and *A. viridis*, which are sister species of *D. muricata* have also been found to effectively express antioxidant activity by suppressing the generation of free radicals such as  $\text{O}_2^-$  (Adegbola et al. 2020).

Mitochondria remain not only as a source of damage-causing free radicals but also as their susceptible target. This in turn stimulates a vicious cycle of excessive ROS generation that damages mitochondrial membrane potential ( $\Delta\Psi\text{m}$ ) and ultimately results in cell death (López et al. 2009). Thus, we studied the mitochondrial membrane potential upon induction with 7KCh and LPS and the possible influence of *D. muricata* on it using Rh123/DAPI staining. Rh123 produced green fluorescence upon sequestration with active mitochondria and DAPI stained the nucleus of every experimented cell in blue colour, irrespective of its health state. Mitochondrial dysfunction and its associated distress-causing signalling cascades are induced by 7KCh and LPS during

pro-inflammatory conditions (Brahmi et al. 2018; Mahalakshmi et al. 2021). M1 and M2 macrophages have been found to exhibit different cellular metabolisms in relation to their polarization and function. Mitochondria have been largely active in M2 macrophages with increased cellular respiration and oxygen consumption to provide its anti-inflammatory property which is inhibited in M1 macrophages. Thus, the regulation of mitochondria is an important factor in the proper management of macrophage polarization and its inflammatory properties (Feng et al. 2018; Qing et al. 2020). Medicinal plant extracts, as well as their active compounds like curcumin (from *Curcuma longa*), TanshinoneIIA (from *Salvia miltiorrhiza*), SO1989 (an oleanolic acid derivative), Guggulsterone (GS from *Commiphora wightii*), etc., have been clinically proven to subside inflammatory responses of M1 macrophages and promote its polarization towards anti-inflammatory phenotype (M2) through the promotion of mitochondrial membrane potential and its function (Cox et al. 2022; Gao et al. 2019; Miller et al. 2019; Yang et al. 2019). Similar results have been obtained in our study where *D. muricata* efficiently prevented mitochondrial damage and retained its membrane potential which was evident from the microscopic images (Fig. 15). We claim from our results that *Digera muricata* being a natural antioxidant was able to exhibit its activity through its protective role of cells and their organelles.

Current evidence suggests that mitochondria-mediated oxidative stress regulates several cellular mechanisms including membrane integrity and death (Prajapati and Gohel 2020). The cytotoxic ability of 7KCh has been reported to disturb plasma membranes by incorporating itself into lipid rafts leading to its condensation (Schieffer et al. 2014). LPS on its own was found to damage macrophage survival resulting in their apoptosis (Conte et al. 2006). These statements have been supported by our results where 7KCh on its own as well as its synergistic effect with LPS were very well able to disrupt the membrane integrity of macrophages even at 24 h resulting in apoptotic events. This process of apoptosis associated with oxidative stress and autophagy was termed “oxiaptophagy” that was appealed to be caused by 7KCh induction (Nury et al. 2014). Several plants and their derivatives generally possess a cytoprotective effect through their primary and secondary metabolites such as oleic acid,  $\alpha$ -tocopherol, terpenoids, phytosterols, resveratrol, etc. (Brahmi et al. 2018). Spinasterol and sitosterols are primary phytosterols of the Mediterranean nutrients which were found to impose cytoprotective activity on 7KCh-induced cytotoxicity (Rezig and Ghzael 2022). The effect of *D. muricata* on the maintenance of membrane integrity (Fig. 16; group IV) against 7KCh and LPS-induced cytotoxicity may potentially be attributed to its phytochemical constituents such as sitosterols. The macrophage cellular damage and death were reported to be



caused by dysfunctional organelles resulting in disrupted calcium homeostasis and hence the calcium mineralization was analysed further in this study.

Abnormal mineralization of calcium in vascular tissues is a common finding in patients with atherosclerosis and is used as a diagnostic marker. Dysfunctional calcification in macrophages is found to be a trigger for pro-inflammatory responses with a spectrum of effects such as matrix metalloprotease production which poses a threat to the severity of atherosclerosis (Ewence et al. 2008). Henceforth, we aimed to check whether a similar response is also produced upon 7KCh treatment in macrophages using an intracellular calcium staining procedure with alizarin red S. The assay result disclosed that the cells treated with 7KCh with or without LPS eventually resulted in increased calcium deposits, thus providing evidence for the role of 7KCh and LPS on uncharacteristic mineralization. On the other hand, co-treatment of the macrophages along with *D. muricata* extract brought the condition back to a standard level with significantly lower calcium deposits similar to control cells (Fig. 17). In support to our findings, suppression of 7KCh-induced apoptosis of cells was shown evidently by the treatment of a phytochemical through prevention of increased intracellular calcium deposition (Tesoriere et al. 2013).

In order to further study the atheroprotective effect of *D. muricata* leaf extract, we tested its ability to check on the levels of gene expression of mediators that result in an inflammatory response. Recent studies have revealed that macrophages possess a hallmark feature of plasticity and can undergo a dynamic transition between M1 and M2 phenotype due to polarization and inflammatory markers-producing genes including iNOS, COX-2, MMP9, IL-1 $\beta$ , IL-6, MRC1 and PPAR $\gamma$  and surface markers such as CD16 and CD36 may serve a key role in macrophage polarization (Zhou et al. 2017). In response to inflammatory stimuli by LPS, M1 phenotypic macrophages produce inducible nitric oxide synthase (iNOS) which uses a substrate like L-arginine to produce nitric oxide (Weisser et al. 2013). Pro-atherogenic enzymes such as iNOS, COX-2 and MMP-9 were assessed for their expression initially (Fig. 18). iNOS generally produces a higher amount of nitric oxide than eNOS and nNOS which could play a role in cellular damage and inflammation (Luoma et al. 1998). The *D. muricata* extract greatly downregulated the expression of iNOS which was induced upon 7KCh and LPS treatment. LPS-treated macrophages stimulate iNOS expression and are sufficient to induce NO synthesis at the transcriptional level (Panaro et al. 2003). Similarly, Gargiulo et al. (2018) in his research concluded that iNOS is upregulated with the induction of oxysterols. Hori et al. (2001) proved that the level of expression of COX-2 is increased or is upregulated during the treatment with LPS through their experiments. COX-2 was upregulated during the treatment with oxysterols (Gargiulo et al.

2018). In contrast, the *D. muricata* extract downregulated the expression of COX-2. Oxysterols in atherosclerotic lesions promote the expression of MMP-9 and contribute to vulnerable plaque (Gargiulo et al. 2011). MMP-9 is associated with the development of cardiovascular diseases and is upregulated by the induction of LPS (Cheng et al. 2009). On the co-treatment with *D. muricata* extract, the expression of MMP-9 was remarkably downregulated.

IL-6 and IL-1 $\beta$  are pro-atherogenic cytokines that are known to be highly secreted during lesion formation. IL-6 is a pro-inflammatory cytokine and is upregulated with the induction of LPS and oxysterol such as 7KCh (Sung et al. 2009; Qi et al. 2019). Supplementation of *Amaranthus cruentus* belonging to *Amaranthaceae* has been found to significantly reduce the expression of inflammatory IL-6 in murine macrophages (Tyszka-Czochara et al. 2016). IL-1 $\beta$  is a key mediator of the inflammatory response which is upregulated by the treatment with LPS and oxysterols (Wong et al. 2020). Similar to this, our results denote that these pro-atherogenic cytokines were expressed highly upon 7KCh and LPS treatment, whereas co-treatment with extract of *D. muricata* notably reduced their expression (Fig. 18).

Scavenging receptors like CD36 and CD163 involve in the excessive uptake of Ox-LDL which results in foam cell formation and expression of M1-like features by M2 macrophages. CD36 is a scavenger receptor that plays a vital role in foam cell formation and is upregulated with the induction of oxysterols such as 7KCh (Leonarduzzi et al. 2006). LPS treatment was also found to increase the mRNA level of CD36 that upregulated the lipid accumulation in macrophages (Li et al. 2013). CD163 is a scavenger receptor expressed by the stimulation of anti-inflammatory mediators and interleukins are upregulated with the induction of LPS and oxysterols (Weaver et al. 2007; Zizzo and Cohen 2015). CD163 was considered to be atheroprotective, whereas a recent discovery shows that it is associated with increased atherosclerotic plaque vulnerability (Bengtsson et al. 2020). They were expressed in increased levels upon treatment with 7KCh along with or without LPS, whereas in contrast they were very much decreased upon co-treatment with *D. muricata* methanol extract (Fig. 18).

Mannose receptor C-type 1, a protein-coding gene highly expressed in M2 macrophages was downregulated by the induction of LPS and oxysterols (Liu et al. 2015; Viaud et al. 2018). Similarly, peroxisome proliferator-activated receptor gamma is an anti-inflammatory enzyme that was downregulated by the induction of oxysterol and LPS (Kim et al. 2007; Ma et al. 2013a, b). Our results provided us with a reasonable indication of *D. muricata* extract to effectively upregulate these anti-atherogenic markers which were downregulated by 7KCh with or without LPS (Fig. 18).

In addition, to study the efficacy of *D. muricata* in maintaining the M2 phenotype of macrophages, TGF $\beta$ 1

expressions were estimated using ELISA. Our study shows that 7KCh reduced the production of TGF $\beta$ 1 in macrophages which supports the previous reports where this particular anti-inflammatory cytokine was reduced by 7KCh to promote pro-inflammatory signalling (Saha and Profumo 2020). Increasing TGF  $\beta$ 1 using phytocompounds such as  $\alpha$ -mangostin, asiaticoside, madecassoside, etc. in macrophages has been found to increase the stability of atherosclerotic plaque by promoting the M2 population (Smedbakken et al. 2012; John et al. 2022; Bandopadhyay et al. 2023). The results of the study are supportive of the previous findings where TGF  $\beta$ 1 concentrations that were reduced upon 7KCh and 7KCh + LPS treatment (Fig. 19; Group II and III) were significantly increased upon co-treatment with *D. muricata* extract. This made us further study its potential in regulating NF- $\kappa$ B and iNOS expression in macrophages. NF- $\kappa$ B is a pro-inflammatory transcription factor that acts as a fundamental controller of the expression of most inflammatory outcomes. Its increase during atherogenesis is attributed to the polarization of macrophages towards the M1 phenotype under chronic diseases and regulating this signalling modulates the plasticity of macrophages (Silveira et al. 2016). Previous studies have shown the phosphorylation and translocation of the transcription factor, NF- $\kappa$ B p65 into the nucleus during abnormal polarization in macrophages with elevated expression of iNOS and its associated pro-atherogenic mediators (He et al. 2017). Plants and phytocompounds such as *Sutherlandia frutescens*, resveratrol, berberine, quercetin and silymarin (Camille and Dealtry 2018; Li and Feng 2020; Bellavite et al. 2023) were reported to influence the regulation of macrophage polarization via NF- $\kappa$ B signalling and similar observation in our immunocytochemistry analysis support the activity of *D. muricata* in preventing macrophage polarization towards pro-inflammatory outcomes (Fig. 20; Group IV). Similar results were observed when iNOS expression was analysed which act as a supplementary indication of preventing abnormal macrophage polarization (Fig. 20; Group IV). Therefore, it is evident from the obtained results that *D. muricata* leaf extract is a possible anti-atherogenic agent against 7KCh and LPS-mediated inflammatory responses.

## Conclusion

In conclusion, sitosterol-rich *D. muricata* extract showed the presence of diverse ethnopharmacologically significant phytochemicals with multiple therapeutic applications making it worthy of functional analyses. We elucidated the atheroprotective property of *Digera muricata* extract in modulating the macrophage polarization and atherogenic responses stimulated by the synergistic effect of 7-ketocholesterol and

bacterial lipopolysaccharide. Deleterious atherosclerotic manifestations in macrophages such as cellular oxidants (NO, ROS and O<sub>2</sub><sup>-</sup>) mitochondrial membrane damage, loss of cellular membrane integrity, reduced pinocytosis, intracellular lipid accumulation and calcium deposition were significantly stabilized by *D. muricata* with increased arginase enzyme activity. Decreased gene expression of pro-atherogenic mediators (iNOS, COX-2, MMP9, IL-6, IL-1 $\beta$ , CD36 and CD163) and increased anti-atherogenic mediators (MRC1 and PPAR $\gamma$ ) in macrophages were imposed by *D. muricata* treatment. This effect may be incurred by the extract as it is sitosterol-rich, a phytosterol with a wide spectrum of medicinal applications. Recently, sitosterol has been explored in many studies owing to its ability in attenuating atherosclerosis and its inflammatory mechanisms. The macrophage polarization phenomenon from anti-inflammatory towards pro-inflammatory phenotype upon 7KCh and LPS stimulation was indirectly confirmed in this study through the determination of inflammatory mediators that are specific for particular macrophage phenotypes. Direct evidence for macrophage polarization is a limitation of this study which will be addressed in future analyses. Nevertheless, particular bioactive compounds which are responsible for this potential activity will be isolated, and characterized and their functional analyses will be investigated in the near future. Thereby, we conclude for the first time that sitosterol-rich *Digera muricata* help in attenuating atherosclerosis development since it was proven to effectively regulate oxysterol-induced macrophage polarization mediators and their atherogenic responses. The inclusion of this medicinal plant in our daily routine diet will be of immense benefit to prevent the manifestation of cardiovascular ailments associated with an unhealthy lifestyle.

**Acknowledgements** We acknowledge the Department of Zoology, University of Madras, Guindy Campus for providing all the support and necessary facilities for performing this study. We greatly acknowledge UGC for providing financial assistance to the research fellow.

**Author contributions** SR conceptualized, performed all the methodologies and compiled the data. PD, MK and LCM assisted in data curation and literature writing. MR and BM provided resources, supervision and validation for the research work. The manuscript has been read and approved for submission by all the authors.

**Funding** The authors did not receive support from any organization for the submitted work.

## Declarations

**Conflict of interest** The authors declare that they have no conflict of interest in the publication.

**Research involving human participants and/or animals** Research does not involve human participants and/or animals.

**Informed consent** Not applicable.

## References

- Adegbola PI, Adetutu A et al (2020) Antioxidant activity of Amaranthus species from the Amaranthaceae family—a review. *S Afr J Bot* 1(133):111–117. <https://doi.org/10.1016/j.sajb.2020.07.003>
- Afrin S, Gasparrini M et al (2018) Protective effects of Manuka honey on LPS-treated RAW 264.7 macrophages. Part 1: enhancement of cellular viability, regulation of cellular apoptosis and improvement of mitochondrial functionality. *Food Chem Toxicol* 1(121):203–213. <https://doi.org/10.1016/j.fct.2018.09.001>
- Al Obaydi MF, Hamed WM et al (2020) *Terfezia boudieri*: a desert truffle with anticancer and immunomodulatory activities. *Front Nutr* 8(7):38. <https://doi.org/10.3389/fnut.2020.00038>
- Anderson A, Campo A et al (2020) 7-Ketocholesterol in disease and aging. *Redox Biol* 1(29):101380. <https://doi.org/10.1016/j.redox.2019.101380>
- Arulmathi R, Sudarmani DN et al (2017) Screening and evaluation of invasive weeds against *Pseudomonas aeruginosa* (Mtcc 3541) for quorum sensing interference and its free radical scavenging. *Res J Pharm Technol* 10(2):525–528. <https://doi.org/10.5958/0974-360X.2017.00104.4>
- Astuti SM, Sakinah MA et al (2011) Determination of saponin compound from *Anredera cordifolia* (Ten) Steenis plant (binahong) to potential treatment for several diseases. *J Agric Sci* 3(4):224. <https://doi.org/10.5539/jas.v3n4p224>
- Bandopadhyay S, Mandal S et al (2023) Therapeutic properties and pharmacological activities of asiaticoside and madecassoside: a review. *J Cell Mol Med* 27(5):593–608. <https://doi.org/10.1111/jcmm.17635>
- Bannerman DD, Goldblum SE (2003) Mechanisms of bacterial lipopolysaccharide-induced endothelial apoptosis. *Am J Physiol Lung Cell Mol Physiol* 284(6):L899–914. <https://doi.org/10.1152/ajplung.00338.2002>
- Barrett TJ (2020) Macrophages in atherosclerosis regression. *Arterioscler Thromb Vasc Biol* 40(1):20–33. <https://doi.org/10.1161/ATVBAHA.119.312802>
- Bellavite P, Fazio S et al (2023) A Descriptive review of the action mechanisms of berberine, quercetin and silymarin on insulin resistance/hyperinsulinemia and cardiovascular prevention. *Molecules* 28(11):4491. <https://doi.org/10.3390/molecules28114491>
- Bengtsson E, Hultman K et al (2020) CD163+ macrophages are associated with a vulnerable plaque phenotype in human carotid plaques. *Sci Rep* 10(1):1–9. <https://doi.org/10.1038/s41598-020-71110-x>
- Bergheanu SC, Bodde MC et al (2017) Pathophysiology and treatment of atherosclerosis. *Neth Heart J* 25(4):231–242. <https://doi.org/10.1007/s12471-017-0959-2>
- Berthier A, Lemaire-Ewing S et al (2005) 7-Ketocholesterol-induced apoptosis: involvement of several pro-apoptotic but also anti-apoptotic calcium-dependent transduction pathways. *FEBS J* 272(12):3093–3104. <https://doi.org/10.1111/j.1742-4658.2005.04723.x>
- Bharath B, Perinbam K et al (2021) Evaluation of the anticancer potential of Hexadecanoic acid from brown algae *Turbinaria ornata* on HT-29 colon cancer cells. *J Mol Struct* 5(1235):130229. <https://doi.org/10.1016/j.molstruc.2021.130229>
- Biasi F, Leonarduzzi G et al (2004) Oxysterol mixtures prevent proapoptotic effects of 7-ketocholesterol in macrophages: implications for proatherogenic gene modulation. *FASEB J* 18(6):693–695. <https://doi.org/10.1096/fj.03-0401fje>
- Boscá L, Zeini M et al (2005) Nitric oxide and cell viability in inflammatory cells: a role for NO in macrophage function and fate. *Toxicology* 208(2):249–258. <https://doi.org/10.1016/j.tox.2004.11.035>
- Brahmi F, Nury T et al (2018) Evaluation of antioxidant, anti-inflammatory and cytoprotective properties of ethanolic mint extracts from Algeria on 7-ketocholesterol-treated murine RAW 264.7 macrophages. *Antioxidants* 7(12):184. <https://doi.org/10.3390/antiox7120184>
- Brahmi F, Vejux A et al (2019) Prevention of 7-ketocholesterol-induced side effects by natural compounds. *Crit Rev Food Sci Nutr* 59(19):3179–3198. <https://doi.org/10.1080/10408398.2018.1491828>
- Brand-Williams W, Cuvelier ME et al (1995) Use of a free radical method to evaluate antioxidant activity. *LWT Food Sci Technol* 28(1):25–30. [https://doi.org/10.1016/S0023-6438\(95\)80008-5](https://doi.org/10.1016/S0023-6438(95)80008-5)
- Bryman A, Cramer D (2012) Quantitative data analysis with IBM SPSS 17, 18 & 19: a guide for social scientists. Routledge. <https://doi.org/10.4324/9780203180990>
- Buttari B, Segoni L et al (2013) 7-Oxo-cholesterol potentiates pro-inflammatory signaling in human M1 and M2 macrophages. *Biochem Pharmacol* 86(1):130–137. <https://doi.org/10.1016/j.bcp.2013.04.008>
- Calle P, Muñoz A et al (2019) CPT1a gene expression reverses the inflammatory and anti-phagocytic effect of 7-ketocholesterol in RAW264.7 macrophages. *Lipids Health Dis* 18(1):1–10. <https://doi.org/10.1186/s12944-019-1156-7>
- Camille N, Dealtry G (2018) Regulation of M1/M2 macrophage polarization by *Sutherlandia frutescens* via NFκB and MAPK signaling pathways. *S Afr J Bot* 116:42–51. <https://doi.org/10.1016/j.sajb.2018.02.400>
- Cathcart MK (2004) Regulation of superoxide anion production by NADPH oxidase in monocytes/macrophages: contributions to atherosclerosis. *Arterioscler Thromb Vasc Biol* 24(1):23–28. <https://doi.org/10.1161/01.ATV.0000097769.47306.12>
- Chang YC, Huang KX et al (2006) Hibiscus anthocyanins-rich extract inhibited LDL oxidation and oxLDL-mediated macrophages apoptosis. *Food Chem Toxicol* 44(7):1015–1023. <https://doi.org/10.1016/j.fct.2005.12.006>
- Cheng YC, Chen LM et al (2009) Lipopolysaccharide upregulates uPA, MMP-2 and MMP-9 via ERK1/2 signaling in H9c2 cardiomyoblast cells. *Mol Cell Biochem* 325(1):15–23. <https://doi.org/10.1007/s11010-008-0016-y>
- Chinetti-Gbaguidi G, Colin S et al (2015) Macrophage subsets in atherosclerosis. *Nat Rev Cardiol* 12(1):10–17. <https://doi.org/10.1038/nrcardio.2014.173>
- Choe SH, Choi EY et al (2019) Telmisartan, an angiotensin II receptor blocker, attenuates Prevotella intermedia lipopolysaccharide-induced production of nitric oxide and interleukin-1β in murine macrophages. *Int Immunopharmacol* 75:105750. <https://doi.org/10.1016/j.intimp.2019.105750>
- Colin S, Chinetti-Gbaguidi G et al (2014) Macrophage phenotypes in atherosclerosis. *Immunol Rev* 262(1):153–166. <https://doi.org/10.1111/imr.12218>
- Conte D, Holcik M et al (2006) Inhibitor of apoptosis protein cIAP2 is essential for lipopolysaccharide-induced macrophage survival. *Mol Cell Biol* 26(2):699–708. <https://doi.org/10.1128/MCB.26.2.699-708.2006>
- Coquette A, Vray B et al (1986) Role of vitamin E in the protection of the resident macrophage membrane against oxidative damage. *Arch Int Physiol Biochim Biophys* 94(5):S29–S34
- Cox FF, Misiou A et al (2022) Protective effects of curcumin in cardiovascular diseases—impact on oxidative stress and mitochondria. *Cells* 11(3):342. <https://doi.org/10.3390/cells11030342>
- Daniel G, Krishnakumari S (2015) Quantitative analysis of primary and secondary metabolites in aqueous hot extract of *Eugenia uniflora* (L) leaves. *Asian J Pharm Clin Res* 8(1):334–338

- de Medina P, Paillasse MR et al (2009) Synthesis of new alkylaminooxysterols with potent cell differentiating activities: identification of leads for the treatment of cancer and neurodegenerative diseases. *J Med Chem* 52(23):7765–7777. <https://doi.org/10.1021/jm901063e>
- Deepthi S, Elumalai P et al (2021) Evaluation of cytotoxic potential of *Digera muricata* leaf extract on lung cancer cell line. *J Pharm Res Int* 29:285–293. <https://doi.org/10.9734/jpri/2021/v33i63A35632>
- Drvar V, Legović D et al (2022) POS0407 oxysterol 7-ketocholesterol can re-program synovial tissue macrophages and support m1 polarization. *Ann Rheum Dis*. <https://doi.org/10.1136/annrheumdis-2022-eular.4042>
- Duraisamy P, Ravi S et al (2022) Dynamic role of macrophage subtypes on development of atherosclerosis and potential use of herbal immunomodulators as imminent therapeutic strategy. *Cardiovasc Hematol Agents Med Chem* 20(1):2–12. <https://doi.org/10.2174/1871525718666201217163207>
- Duraisamy P, Ravi S et al (2023) *Scoparia dulcis* and *Indigofera tinctoria* as potential herbal remedies against 7-ketocholesterol-induced pro-inflammatory mediators of macrophage polarization. *J Herb Med* 39:100652. <https://doi.org/10.1016/j.hermed.2023.100652>
- Elgailani IE (2018) Spectrophotometric analysis of some metals and phytochemical screening of *Digera muricata* (leaves and stems). *Pak J Pharm Sci* 31(5):1923–1926
- Ewence AE, Bootman M et al (2008) Calcium phosphate crystals induce cell death in human vascular smooth muscle cells: a potential mechanism in atherosclerotic plaque destabilization. *Circ Res* 103(5):e28–34. <https://doi.org/10.1161/CIRCRESAHA.108.181305>
- Feng J, Li L et al (2018) IL-25 stimulates M2 macrophage polarization and thereby promotes mitochondrial respiratory capacity and lipolysis in adipose tissues against obesity. *Cell Mol Immunol* 15(5):493–505. <https://doi.org/10.1038/cmi.2016.71>
- Forbes-Hernández TY, Giampieri F (2014) The effects of bioactive compounds from plant foods on mitochondrial function: a focus on apoptotic mechanisms. *Food Chem Toxicol* 68:154–182. <https://doi.org/10.1016/j.fct.2014.03.017>
- Förstermann U, Xia N et al (2017) Roles of vascular oxidative stress and nitric oxide in the pathogenesis of atherosclerosis. *Circ Res* 120(4):713–735. <https://doi.org/10.1161/CIRCRESAHA.116.309326>
- Frostegård J (2013) Immunity, atherosclerosis and cardiovascular disease. *BMC Med* 11(1):1–3. <https://doi.org/10.1186/1741-7015-11-117>
- Gao S, Wang Y et al (2019) Tanshinone IIA alleviates inflammatory response and directs macrophage polarization in lipopolysaccharide-stimulated RAW264.7 cells. *Inflammation* 42(1):264–275. <https://doi.org/10.1007/s10753-018-0891-7>
- Gargiulo S, Sottero B et al (2011) Plaque oxysterols induce unbalanced up-regulation of matrix metalloproteinase-9 in macrophagic cells through redox-sensitive signaling pathways: implications regarding the vulnerability of atherosclerotic lesions. *Free Radic Biol Med* 51(4):844–855. <https://doi.org/10.1016/j.freeradbiomed.2011.05.030>
- Gargiulo S, Rossin D et al (2018) Up-regulation of COX-2 and mPGES-1 by 27-hydroxycholesterol and 4-hydroxynonal: a crucial role in atherosclerotic plaque instability. *Free Radic Biol Med* 129:354–363. <https://doi.org/10.1016/j.freeradbiomed.2018.09.046>
- Geetha TS, Geetha N (2014) Phytochemical screening, quantitative analysis of primary and secondary metabolites of *Cymbopogon citratus* (DC) Stapf. leaves from Kodaikanal hills, Tamilnadu. *Int J Pharmtech Res* 6(2):521–529
- Gelissen IC, Brown AJ et al (1996) Sterol efflux is impaired from macrophage foam cells selectively enriched with 7-ketocholesterol. *J Biol Chem* 271(30):17852–17860. <https://doi.org/10.1074/jbc.271.30.17852>
- Ghaffar A, Tung BT et al (2019) Botanical specifications, chemical composition and pharmacological applications of tartara (*Digera muricata* L.)—a review. *Int J Chem Biochem Sci* 16:17–22
- Ghosh B (1999) Quercetin inhibits LPS-induced nitric oxide and tumor necrosis factor- $\alpha$  production in murine macrophages. *Int Immunopharmacol* 21(7):435–443. [https://doi.org/10.1016/S0192-0561\(99\)00024-7](https://doi.org/10.1016/S0192-0561(99)00024-7)
- Gomathi D, Kalaiselvi M et al (2015) GC-MS analysis of bioactive compounds from the whole plant ethanolic extract of *Evolvulus alsinoides* (L.) L. *J Food Sci Technol* 52(2):1212–1217. <https://doi.org/10.1007/s13197-013-1105-9>
- Gregory CA, McNeill EP et al (2020) Preparation of osteogenic matrices from cultured cells. *Methods Cell Biol* 156:15–43. <https://doi.org/10.1016/bs.mcb.2019.10.009>
- Gulluce M, Sahin F et al (2007) Antimicrobial and antioxidant properties of the essential oils and methanol extract from *Mentha longifolia* L. ssp. longifolia. *Food Chem* 103(4):1449–1456. <https://doi.org/10.1016/j.foodchem.2006.10.061>
- Gupta R, Sharma AK et al (2011) Antidiabetic and antioxidant potential of  $\beta$ -sitosterol in streptozotocin-induced experimental hyperglycemia. *J Diabetes* 3(1):29–37. <https://doi.org/10.1111/j.1753-0407.2010.00107.x>
- Gylling H, Plat J et al (2014) Plant sterols and plant stanols in the management of dyslipidaemia and prevention of cardiovascular disease. *Atherosclerosis* 232(2):346–360. <https://doi.org/10.1016/j.atherosclerosis.2013.11.043>
- Hayden JM, Brachova L et al (2002) Induction of monocyte differentiation and foam cell formation *in vitro* by 7-ketocholesterol. *J Lipid Res* 43(1):26–35
- He Y, Ma X et al (2017) Thiamet G mediates neuroprotection in experimental stroke by modulating microglia/macrophage polarization and inhibiting NF- $\kappa$ B p65 signaling. *J Cereb Blood Flow Metab* 37(8):2938–2951. <https://doi.org/10.1177/0271678X16679671>
- Henry GE, Momin RA et al (2002) Antioxidant and cyclooxygenase activities of fatty acids found in food. *J Agric Food Chem* 50(8):2231–2234. <https://doi.org/10.1021/jf0114381>
- Hori M, Kita M et al (2001) Upregulation of iNOS by COX-2 in muscularis resident macrophage of rat intestine stimulated with LPS. *Am J Physiol Gastrointest Liver Physiol* 280(5):G930–G938. <https://doi.org/10.1152/ajpgi.2001.280.5.G930>
- Huang Z, Liu Q et al (2010) 7-Ketocholesterol induces cell apoptosis by activation of nuclear factor kappa B in mouse macrophages. *Acta Med Okayama* 64(2):85–93. <https://doi.org/10.18926/AMO/32848>
- Jagatha G, Senthilkumar N (2011) Evaluation of anti-diabetic activity of methanol extract of *Digera muricata* (L) mart in alloxan induced diabetic rats. *Int J Pharm Sci Res* 2(6):748–752. [https://doi.org/10.13040/IJPSR.0975-8232.2\(6\).1525-29](https://doi.org/10.13040/IJPSR.0975-8232.2(6).1525-29)
- John S, Priyadarshini S et al (2017) Phytochemical profile and thin layer chromatographic studies of *Daucus carota* peel extracts. *Int J Food Sci Nutr* 2(1):23–26
- John OD, Mushunje AT et al (2022) The metabolic and molecular mechanisms of  $\alpha$  mangostin in cardiometabolic disorders. *Int J Mol Med* 50(3):1–37. <https://doi.org/10.3892/ijmm.2022.5176>
- Johnson LV, Walsh ML et al (1980) Localization of mitochondria in living cells with rhodamine 123. *Proc Natl Acad Sci USA* 77(2):990–994. <https://doi.org/10.1073/pnas.77.2.990>
- Jung CH, Jun CY et al (2006) *Rhus verniciflua* stokes extract: radical scavenging activities and protective effects on H<sub>2</sub>O<sub>2</sub>-induced cytotoxicity in macrophage RAW 264.7 cell lines. *Biol Pharm Bull* 29(8):1603–1607. <https://doi.org/10.1248/bpb.29.1603>

- Kabesh K, Senthilkumar P et al (2015) Phytochemical analysis of *Catharanthus roseus* plant extract and its antimicrobial activity. *Int J Pure Appl Biosci* 3(2):162–172. <https://doi.org/10.18782/2582-2845>
- Kaplan M, Hayek T et al (2001) Pomegranate juice supplementation to atherosclerotic mice reduces macrophage lipid peroxidation, cellular cholesterol accumulation and development of atherosclerosis. *J Nutr* 131(8):2082–2089. <https://doi.org/10.1093/jn/131.8.2082>
- Kattoor AJ, Pothineni NV et al (2017) Oxidative stress in atherosclerosis. *Curr Atheroscler Rep* 19(11):1–11. <https://doi.org/10.1007/s11883-017-0678-6>
- Khallou-Laschet J, Varthaman A et al (2010) Macrophage plasticity in experimental atherosclerosis. *PLoS One* 5(1):e8852. <https://doi.org/10.1371/journal.pone.0008852>
- Khan MR, Ahmed D (2009) Protective effects of *Digera muricata* (L.) Mart. on testis against oxidative stress of carbon tetrachloride in rat. *Food Chem Toxicol* 47(6):1393–1399. <https://doi.org/10.1016/j.fct.2009.03.020>
- Khan MR, Younus T (2011) Prevention of CCl<sub>4</sub>-induced oxidative damage in adrenal gland by *Digera muricata* extract in rat. *Pak J Pharm Sci* 24(4):469–473
- Khan MR, Rizvi W et al (2009) Carbon tetrachloride-induced nephrotoxicity in rats: protective role of *Digera muricata*. *J Ethnopharmacol* 122(1):91–99. <https://doi.org/10.1016/j.jep.2008.12.006>
- Khan MR, Afzaal M et al (2011a) Protective potential of methanol extract of *Digera muricata* on acrylamide induced hepatotoxicity in rats. *Afr J Biotechnol* 10(42):8456–8464. <https://doi.org/10.5897/AJB11.771>
- Khan MR, Khan GN et al (2011b) Evaluation of antioxidant and fertility effects of *Digera muricata* in male rats. *Afr J Pharm Pharmacol* 5(6):688–699. <https://doi.org/10.5897/AJPP.9000147>
- Kim WK, Meliton V et al (2007) 20 (S)-hydroxycholesterol inhibits PPAR $\gamma$  expression and adipogenic differentiation of bone marrow stromal cells through a hedgehog-dependent mechanism. *J Bone Miner Res* 22(11):1711–1719. <https://doi.org/10.1359/jbmr.070710>
- Kirichenko TV, Sukhorukov VN et al (2020) Medicinal plants as a potential and successful treatment option in the context of atherosclerosis. *Front Pharmacol* 11:403. <https://doi.org/10.3389/fphar.2020.00403>
- Kraus NA, Rudolphi B et al (2016) Valid assessment of lipid content of cultured adipocytes using oil red O. *Diabetologie* 11(S 01):P228. <https://doi.org/10.1055/s-0036-1580975>
- Kruth HS (2011) Receptor-independent fluid-phase pinocytosis mechanisms for induction of foam cell formation with native LDL particles. *Curr Opin Lipidol* 22(5):386. <https://doi.org/10.1097/MOL.0b013e32834adadb>
- Larsson H, Böttiger Y et al (2007) *In vivo* interconversion of 7 $\beta$ -hydroxycholesterol and 7-ketocholesterol, potential surrogate markers for oxidative stress. *Free Radic Biol Med* 43(5):695–701. <https://doi.org/10.1016/j.freeradbiomed.2007.04.033>
- Leonarduzzi G, Vizio B et al (2006) Early involvement of ROS overproduction in apoptosis induced by 7-ketocholesterol. *Antioxid Redox Signal* 8(3–4):375–380. <https://doi.org/10.1089/ars.2006.8.375>
- Li AC, Glass CK (2002) The macrophage foam cell as a target for therapeutic intervention. *Nat Med* 8(11):1235–1242. <https://doi.org/10.1038/nm1102-1235>
- Li H, Horke S (2014) Vascular oxidative stress, nitric oxide and atherosclerosis. *Atherosclerosis* 237(1):208–219. <https://doi.org/10.1016/j.atherosclerosis.2014.09.001>
- Li XY, Wang C et al (2013) *Porphyromonas gingivalis* lipopolysaccharide increases lipid accumulation by affecting CD36 and ATP-binding cassette transporter A1 in macrophages. *Oncol Rep* 30(3):1329–1336. <https://doi.org/10.3892/or.2013.2600>
- Li Y, Feng L et al (2020) Resveratrol prevents ISO-induced myocardial remodeling associated with regulating polarization of macrophages through VEGF-B/AMPK/NF- $\kappa$ B pathway. *Int Immunopharmacol* 84:106508. <https://doi.org/10.1016/j.intimp.2020.106508>
- Libby P, Ridker PM et al (2009) Leducq transatlantic network on atherothrombosis. Inflammation in atherosclerosis: from pathophysiology to practice. *J Am Coll Cardiol* 54(23):2129–2138. <https://doi.org/10.1016/j.jacc.2009.09.009>
- Liu RH (2003) Health benefits of fruit and vegetables are from additive and synergistic combinations of phytochemicals. *Am J Clin Nutr* 78(3):517S–520S. <https://doi.org/10.1093/ajcn/78.3.517S>
- Liu J, Zhao D et al (2015) Prion protein participates in the protection of mice from lipopolysaccharide infection by regulating the inflammatory process. *J Mol Neurosci* 55(1):279–287. <https://doi.org/10.1007/s12031-014-0319-2>
- Liu Y, Wang X et al (2018) Attenuation of atherosclerosis by protocatechuic acid via inhibition of M1 and promotion of M2 macrophage polarization. *J Agric Food Chem* 67(3):807–818. <https://doi.org/10.1021/acs.jafc.8b05719>
- Liu S, Lu Z et al (2022) *Castanea mollissima* shell polyphenols regulate JAK2 and PPAR $\gamma$  expression to suppress inflammation and lipid accumulation by inhibiting M1 macrophages polarization. *J Funct Foods* 92:105046. <https://doi.org/10.1016/j.jff.2022.105046>
- López A, García JA et al (2009) Melatonin protects the mitochondria from oxidative damage reducing oxygen consumption, membrane potential, and superoxide anion production. *J Pineal Res* 46(2):188–198. <https://doi.org/10.1111/j.1600-079X.2008.00647.x>
- Lopukhov AV, Yang Z et al (2021) Mannosylated cationic copolymers for gene delivery to macrophages. *Macromol Biosci* 21(4):2000371. <https://doi.org/10.1002/mabi.202000371>
- Luoma JS, Strålin P et al (1998) Expression of extracellular SOD and iNOS in macrophages and smooth muscle cells in human and rabbit atherosclerotic lesions: colocalization with epitopes characteristic of oxidized LDL and peroxynitrite-modified proteins. *Arterioscler Thromb Vasc Bio* 18(2):157–167. <https://doi.org/10.1161/01.atv.18.2.157>
- Ma GC, Wu PF et al (2013a) Inhibitory effect of Piper betel leaf extracts on copper-mediated LDL oxidation and oxLDL-induced lipid accumulation via inducing reverse cholesterol transport in macrophages. *Food Chem* 141(4):3703–3713. <https://doi.org/10.1016/j.foodchem.2013.06.003>
- Ma Z, Ji W et al (2013b) Formononetin inhibited the inflammation of LPS-induced acute lung injury in mice associated with induction of PPAR gamma expression. *Inflammation* 36(6):1560–1566. <https://doi.org/10.1007/s10753-013-9700-5>
- Madhu CS, Manukumar HM et al (2014) New-vista in finding antioxidant and anti-inflammatory property of crude protein extract from *Sauropus androgynus* leaf. *Acta Sci Pol Technol Aliment* 13(4):375–383. <https://doi.org/10.17306/J.AFS.2014.4.4>
- Mahalakshmi K, Parimalanandhini D et al (2021) Influential role of 7-Ketocholesterol in the progression of Alzheimer's disease. *Prostaglandins Other Lipid Mediat* 156:106582. <https://doi.org/10.1016/j.prostaglandins.2021.106582>
- Manikandan R, Beulaja M et al (2017) Biosynthesis of silver nanoparticles using aqueous extract of *Phyllanthus acidus* L. fruits and characterization of its anti-inflammatory effect against H<sub>2</sub>O<sub>2</sub> exposed rat peritoneal macrophages. *Process Biochem* 55:172–181. <https://doi.org/10.1016/j.procbio.2017.01.023>
- Manikandan R, Parimalanandhini D et al (2020) Studies on isolation, characterization of fucoidan from brown algae *Turbinaria decurrens* and evaluation of its in vivo and in vitro

- anti-inflammatory activities. *Int J Biol Macromol* 160:1263–1276. <https://doi.org/10.1016/j.ijbiomac.2020.05.152>
- Marrelli M, De Marco CT et al (2022) Ranunculus species suppress nitric oxide production in LPS-stimulated RAW 264.7 macrophages. *Nat Prod Res* 36(11):2859–2863. <https://doi.org/10.1080/14786419.2021.1920018>
- Martinez FO, Gordon S et al (2006) Transcriptional profiling of the human monocyte-to-macrophage differentiation and polarization: new molecules and patterns of gene expression. *J Immunol* 177(10):7303–7311. <https://doi.org/10.4049/jimmunol.177.10.7303>
- Mathad P, Mety SS (2010) Phytochemical and antimicrobial activity of *Digera muricata* (L.) mart. *J Chem* 7(1):275–280. <https://doi.org/10.1155/2010/509254>
- Mehwish S, Islam A et al (2019) *In vitro* antileishmanial and anti-oxidant potential, cytotoxicity evaluation and phytochemical analysis of extracts from selected medicinally important plants. *Biocatal Agric Biotechnol* 19:101117. <https://doi.org/10.1016/j.bcab.2019.101117>
- Miah MM, Das P et al (2017) Bioactivities of *Digera muricata* (L.) Mart. Available in Bangladesh. *Dhaka Univ J Pharm Sci* 16(2):251–254. <https://doi.org/10.3329/DUJPS.V16I2.35264>
- Miller CN, Samuels JS et al (2019) Guggulsterone activates adipocyte beiging through direct effects on 3T3-L1 adipocytes and indirect effects mediated through RAW264.7 macrophages. *Medicines* 6(1):22. <https://doi.org/10.3390/medicines6010022>
- Monier S, Samadi M et al (2003) Impairment of the cytotoxic and oxidative activities of  $\gamma$ -hydroxycholesterol and 7-ketocholesterol by esterification with oleate. *Biochem Biophys Res Commun* 303(3):814–824. [https://doi.org/10.1016/s0006-291x\(03\)00412-1](https://doi.org/10.1016/s0006-291x(03)00412-1)
- Moore KJ, Tabas I (2011) Macrophages in the pathogenesis of atherosclerosis. *Cell* 145(3):341–355. <https://doi.org/10.1016/j.cell.2011.04.005>
- Moore KJ, Sheedy FJ et al (2013) Macrophages in atherosclerosis: a dynamic balance. *Nat Rev Immunol* 13(10):709–721. <https://doi.org/10.1038/nri3520>
- Moore K, Howard L et al (2019) Inhibitory effects of cranberry polyphenol and volatile extracts on nitric oxide production in LPS activated RAW 264.7 macrophages. *Food Funct* 10(11):7091–7102. <https://doi.org/10.1039/C9FO01500K>
- More GK, Makola RT (2020) *In-vitro* analysis of free radical scavenging activities and suppression of LPS-induced ROS production in macrophage cells by *Solanum sisymbriifolium* extracts. *Sci Rep* 10(1):1–9. <https://doi.org/10.1038/s41598-020-63491-w>
- Mosser DM, Edwards JP (2008) Exploring the full spectrum of macrophage activation. *Nat Rev Immunol* 8(12):958–969. <https://doi.org/10.1038/nri2448>
- Mubark F, Ahmed IM (2020) Chemical evidence supporting the inclusion of Amaranthaceae and Chenopodiaceae into one family Amaranthaceae Juss. (sl). Chief Editor. <https://doi.org/10.36713/epra6001>
- Muhammad RK, Gul NK et al (2011) Evaluation of antioxidant and fertility effects of *Digera muricata* in male rats. *Afr J Pharm Pharmacol* 5(6):688–699. <https://doi.org/10.5897/AJPP.9000147>
- Munder M, Mollinedo F et al (2005) Arginase I is constitutively expressed in human granulocytes and participates in fungicidal activity. *Blood* 105(6):2549–2556. <https://doi.org/10.1182/blood-2004-07-2521>
- Napoli C, Ignarro LJ (2001) Nitric oxide and atherosclerosis. *Nitric Oxide* 5(2):88–97. <https://doi.org/10.1006/niox.2001.0337>
- Napoli C, de Nigris F et al (2006) Nitric oxide and atherosclerosis: an update. *Nitric Oxide* 15(4):265–279. <https://doi.org/10.1016/j.niox.2006.03.011>
- Nathan C, Ding A (2010) Nonresolving inflammation. *Cell* 140(6):871–882. <https://doi.org/10.1016/j.cell.2010.02.029>
- Ning TJ, Yusoff SD et al (2019) Inhibitory effects of *Gynura procumbens* ethanolic extract on nitric oxide production and inducible nitric oxide synthase (iNOS) protein expression in macrophages. *Sains Malays* 48(8):1737–1744. <https://doi.org/10.17576/jsm-2019-4808-20>
- Nury T, Zarrouk A et al (2014) Induction of oxiaoptophagy, a mixed mode of cell death associated with oxidative stress, apoptosis and autophagy, on 7-ketocholesterol-treated 158N murine oligodendrocytes: Impairment by  $\alpha$ -tocopherol. *Biochem Biophys Res Commun* 446(3):714–719. <https://doi.org/10.1016/j.bbrc.2013.11.081>
- O'Brien J, Wilson I et al (2000) Investigation of the Alamar Blue (resazurin) fluorescent dye for the assessment of mammalian cell cytotoxicity. *Eur J Biochem* 267(17):5421–5426. <https://doi.org/10.1046/j.1432-1327.2000.01606.x>
- Ostos MA, Recalde D et al (2002) Implication of natural killer T cells in atherosclerosis development during a LPS-induced chronic inflammation. *FEBS Lett* 519(1–3):23–29. [https://doi.org/10.1016/s0014-5793\(02\)02692-3](https://doi.org/10.1016/s0014-5793(02)02692-3)
- Padwad Y, Ganju L et al (2006) Effect of leaf extract of Seabuckthorn on lipopolysaccharide induced inflammatory response in murine macrophages. *Int Immunopharmacol* 6(1):46–52. <https://doi.org/10.1016/j.intimp.2005.07.015>
- Palozza P, Simone R et al (2010) Lycopene prevents 7-ketocholesterol-induced oxidative stress, cell cycle arrest and apoptosis in human macrophages. *J Nutr Biochem* 21(1):34–46. <https://doi.org/10.1016/j.jnutbio.2008.10.002>
- Panaro MA, Brandonisio O et al (2003) Evidences for iNOS expression and nitric oxide production in the human macrophages. *Current Drug Targets Immune Endocr Metab Immune Disord Drug Targets* 3(3):210–221. <https://doi.org/10.2174/1568008033340216>
- Pascual ME, Carretero ME et al (2002) Simplified screening by TLC of plant drugs. *Pharm Biol* 40(2):139–143. <https://doi.org/10.1076/phbi.40.2.139.5849>
- Patel RP, Levenon AL et al (2000) Mechanisms of the pro-and anti-oxidant actions of nitric oxide in atherosclerosis. *Cardiovasc Res* 47(3):465–474. [https://doi.org/10.1016/s0008-6363\(00\)00086-9](https://doi.org/10.1016/s0008-6363(00)00086-9)
- Patel Shivani S, Nainesh M (2017) Phytochemical screening and estimation of total phenolic and flavonoid content in selected weeds. *Braz J Biol*. <https://doi.org/10.2017/IJRC.2456.6683/202009021>
- Peng X, Chen H et al (2020) Effects of NIX-mediated mitophagy on ox-LDL-induced macrophage pyroptosis in atherosclerosis. *Cell Biol Int* 44(7):1481–1490. <https://doi.org/10.1002/cbin.11343>
- Prajapati P, Gohel D et al (2020) TRIM32 regulates mitochondrial mediated ROS levels and sensitizes the oxidative stress induced cell death. *Cell Signal* 76:109777. <https://doi.org/10.1016/j.cellsig.2020.109777>
- Punchard NA, Whelan CJ et al (2004) The journal of inflammation. *J Inflamm Res* 1(1):1–4. <https://doi.org/10.1186/1476-9255-1-1>
- Qi K, Lin R et al (2019) Long non-coding RNA (lncRNA) CAIF is downregulated in osteoarthritis and inhibits LPS-induced interleukin 6 (IL-6) upregulation by downregulation of miR-1246. *Med Sci Monit* 25:8019. <https://doi.org/10.12659/MSM.917135>
- Qing J, Zhang Z et al (2020) Mitochondrial metabolism in regulating macrophage polarization: an emerging regulator of metabolic inflammatory diseases. *Acta Biochem Biophys Sin* 52(9):917–926. <https://doi.org/10.1093/abbs/gmaa081>
- Ramalashmi K (2019) *In vitro* antidiabetic potential and GC-MS analysis of *Digera muricata* and *Amaranthus cruentus*. *J Med Plants Stud* 7(4):10–16
- Rao X, Zhong J et al (2014) CD36-dependent 7-ketocholesterol accumulation in macrophages mediates progression of atherosclerosis in response to chronic air pollution exposure. *Circ Res* 115(9):770–780. <https://doi.org/10.1161/CIRCRESAHA.115.304666>

- Rasheed A, Azeez RF (2019) A review on natural antioxidants. J Tradit. <https://doi.org/10.5772/intechopen.82636>
- Rath M, Müller I et al (2014) Metabolism via arginase or nitric oxide synthase: two competing arginine pathways in macrophages. Front Immunol 5:532. <https://doi.org/10.3389/fimmu.2014.00532>
- Ravi S, Duraisamy P et al (2021) An insight on 7-ketocholesterol mediated inflammation in atherosclerosis and potential therapeutics. Steroids 172:108854. <https://doi.org/10.1016/j.steroids.2021.108854>
- Rezig L, Ghzaiel I et al (2022) Cytoprotective activities of representative nutrients from the Mediterranean diet and of Mediterranean oils against 7-ketocholesterol-and 7 $\beta$ -hydroxycholesterol-induced cytotoxicity: application to age-related diseases and civilization diseases. Steroids 24:109093. <https://doi.org/10.1016/j.steroids.2022.109093>
- Rodriguez IR, Alam S et al (2004) Cytotoxicity of oxidized low-density lipoprotein in cultured RPE cells is dependent on the formation of 7-ketocholesterol. Invest Ophthalmol vis Sci 45(8):2830–2837. <https://doi.org/10.1167/iovs.04-0075>
- Rosenblat M, Volkova N et al (2013) Pomegranate phytosterol ( $\beta$ -sitosterol) and polyphenolic antioxidant (punicalagin) addition to statin, significantly protected against macrophage foam cells formation. Atherosclerosis 226(1):110–117. <https://doi.org/10.1016/j.atherosclerosis.2012.10.054>
- Roshan MH, Tambo A et al (2016) The role of TLR2, TLR4, and TLR9 in the pathogenesis of atherosclerosis. Int J Inflamm. <https://doi.org/10.1155/2016/1532832>
- Ross R (1986) The pathogenesis of atherosclerosis—an update. N Engl J Med 314(8):488–500. <https://doi.org/10.1056/NEJM198602203140806>
- Ross R (1995) Cell biology of atherosclerosis. Annu Rev Physiol 57:791–804. <https://doi.org/10.1146/annurev.ph.57.030195.004043>
- Rubbo H, Radi R et al (1994) Nitric oxide regulation of superoxide and peroxynitrite-dependent lipid peroxidation. Formation of novel nitrogen-containing oxidized lipid derivatives. J Biol Chem 269(42):26066–26075
- Ryu JH, Ahn H et al (2003) Inhibitory activity of plant extracts on nitric oxide synthesis in LPS-activated macrophages. Phytother Res 17(5):485–489. <https://doi.org/10.1002/ptr.1180>
- Saha S, Profumo E et al (2020) Lupeol counteracts the proinflammatory signalling triggered in macrophages by 7-keto-cholesterol: new perspectives in the therapy of atherosclerosis. Oxid Med Cell Longev. <https://doi.org/10.1155/2020/1232816>
- Salaverry LS, Parrado AC et al (2020) In vitro anti-inflammatory properties of *Smilax campestris* aqueous extract in human macrophages, and characterization of its flavonoid profile. J Ethnopharmacol 247:112282. <https://doi.org/10.1016/j.jep.2019.112282>
- Santos CC, Salvadori MS et al (2013) Antinociceptive and antioxidant activities of phytol *in vivo* and *in vitro* models. J Neurosci. <https://doi.org/10.1155/2013/949452>
- Sarna LK, Wu N et al (2010) Berberine inhibits NADPH oxidase mediated superoxide anion production in macrophages. Can J Physiol Pharmacol 88(3):369–378. <https://doi.org/10.1139/Y09-136>
- Sathiavelu M, Arunachalam S (2012) High performance thin layer chromatography profile of *Cassipoupa filiformis*. Asian Pac J Trop Biomed 2(3):S1431–1435. [https://doi.org/10.1016/S2221-1691\(14\)60224-0](https://doi.org/10.1016/S2221-1691(14)60224-0)
- Schieffler D, Naware S et al (2014) Lipid raft-based membrane order is important for antigen-specific clonal expansion of CD4+ T lymphocytes. BMC Immunol 15(1):1–3. <https://doi.org/10.1186/s12865-014-0058-8>
- Schmid-Schönbein GW (2006) Analysis of inflammation. Annu Rev Biomed Eng 8:93–151. <https://doi.org/10.1146/annurev.bioeng.8.061505.095708>
- Shah R, Shah SA et al (2020) Green synthesis and antibacterial activity of gold nanoparticles of *Digera muricata*. Indian J Pharm Sci 82(2):374–378. <https://doi.org/10.36468/pharmaceutical-sciences.659>
- Shazia U, Arshad H et al (2013) Determination of infochemicals, phytochemical screening and evaluation of antioxidant potential of *Digera muricata*. Der Pharm Lett 5(2):3–4
- Silveira LS, Antunes BD et al (2016) Macrophage polarization: implications on metabolic diseases and the role of exercise. Crit Rev Eukaryot Gene Expr 26(2):115–132. <https://doi.org/10.1615/CritRevEukaryotGeneExpr.2016015920>
- Sim Choi H, Woo Kim J et al (2006) A quantitative nitroblue tetrazolium assay for determining intracellular superoxide anion production in phagocytic cells. J Immunoassay Immunochem 27(1):31–44. <https://doi.org/10.1080/15321810500403722>
- Smedbakken LM, Halvorsen B et al (2012) Increased levels of the homeostatic chemokine CXCL13 in human atherosclerosis-potential role in plaque stabilization. Atherosclerosis 224(1):266–273. <https://doi.org/10.1016/j.atherosclerosis.2012.06.071>
- Smythe CD, Skinner VO et al (2003) The state of macrophage differentiation determines the TNF $\alpha$  response to nitrated lipoprotein uptake. Atherosclerosis 170(2):213–221. [https://doi.org/10.1016/s0021-9150\(03\)00285-5](https://doi.org/10.1016/s0021-9150(03)00285-5)
- Sung SC, Kim K et al (2009) 7-Ketocholesterol upregulates interleukin-6 via mechanisms that are distinct from those of tumor necrosis factor- $\alpha$ , in vascular smooth muscle cells. J Vasc Res 46(1):36–44. <https://doi.org/10.1159/000135663>
- Sur TK, Pandit S et al (2002) Studies on the antiinflammatory activity of *Betula alnoides* bark. Phytother Res 16:669–671. <https://doi.org/10.1002/ptr.942>
- Swirski FK, Pittet MJ et al (2006) Monocyte accumulation in mouse atherosclerosis is progressive and proportional to extent of disease. Proc Natl Acad Sci USA 103(27):10340–10345. <https://doi.org/10.1073/pnas.0604260103>
- Tesorieri L, Attanzio A et al (2013) Phytochemical indicaxanthin suppresses 7-ketocholesterol-induced THP-1 cell apoptosis by preventing cytosolic Ca<sup>2+</sup> increase and oxidative stress. Br J Nutr 110(2):230–240. <https://doi.org/10.1017/S000711451200493X>
- Tiwari M, Dwivedi UN et al (2010) Suppression of oxidative stress and pro-inflammatory mediators by *Cymbopogon citratus* D. Stapf extract in lipopolysaccharide stimulated murine alveolar macrophages. Food Chem Toxicol 48(10):2913–2910. <https://doi.org/10.1016/j.fct.2010.07.027>
- Tyszka-Czochara M, Pasko P et al (2016) Selenium supplementation of amaranth sprouts influences betacyanin content and improves anti-inflammatory properties via NF $\kappa$ B in murine RAW 264.7 macrophages. Biol Trace Elem Res 169(2):320–330. <https://doi.org/10.1007/s12011-015-0429-x>
- Usmani S, Hussain A et al (2013) Pharmacognostical and phytochemical analysis of *Digera muricata* Linn. growing as a weed in fields of Uttar Pradesh region of India. Int J Pharm Pharm Sci 5(1):142–145
- Utley HG, Bernheim F et al (1967) Effect of sulfhydryl reagents on peroxidation in microsomes. Arch Biochem 118(1):29–32. [https://doi.org/10.1016/0003-9861\(67\)90273-1](https://doi.org/10.1016/0003-9861(67)90273-1)
- Vasanthi RH, ShriShriMal N et al (2012) Phytochemicals from plants to combat cardiovascular disease. Curr Med Chem 19(14):2242–2251. <https://doi.org/10.2174/092986712800229078>
- Viaud M, Ivanov S et al (2018) Lysosomal cholesterol hydrolysis couples efferocytosis to anti-inflammatory oxysterol production. Circ Res 122(10):369–384. <https://doi.org/10.1161/CIRCRESAHA.117.312333>
- Vinciguerra M, Romiti S et al (2021) SARS-CoV-2 and atherosclerosis: should COVID-19 be recognized as a new predisposing

- cardiovascular risk factor? *J Cardiovasc Dev Dis* 8(10):130. <https://doi.org/10.3390/jcdd8100130>
- Virgili F, Marino M (2008) Regulation of cellular signals from nutritional molecules: a specific role for phytochemicals, beyond antioxidant activity. *Free Radic Biol Med* 45(9):1205–1216. <https://doi.org/10.1016/j.freeradbiomed.2008.08.001>
- Vivancos M, Moreno JJ (2008) Effect of resveratrol, tyrosol and  $\beta$ -sitosterol on oxidised low-density lipoprotein-stimulated oxidative stress, arachidonic acid release and prostaglandin E2 synthesis by RAW 264.7 macrophages. *Br J Nutr* 99(6):1199–1207. <https://doi.org/10.1017/S0007114507876203>
- Vouldoukis I, Lacan D et al (2004) Antioxidant and anti-inflammatory properties of a *Cucumis melo* LC. extract rich in superoxide dismutase activity. *J Ethnopharmacol* 94(1):67–75. <https://doi.org/10.1016/j.jep.2004.04.023>
- Wang Y, Wang GZ et al (2014) Macrophage mitochondrial oxidative stress promotes atherosclerosis and nuclear factor- $\kappa$ B-mediated inflammation in macrophages. *Circ Res* 114(3):421–433. <https://doi.org/10.1161/CIRCRESAHA.114.302153>
- Weaver LK, Pioli PA et al (2007) Up-regulation of human monocyte CD163 upon activation of cell-surface Toll-like receptors. *J Leukoc Biol* 81(3):663–671. <https://doi.org/10.1189/jlb.0706428>
- Weisser SB, McLaren KW et al (2013) Generation and characterization of murine alternatively activated macrophages. In: Helgason CD, Miller CL (eds) *Basic cell culture protocols*. Humana Press, Totowa, NJ, pp 225–239
- Wong MY, Lewis M et al (2020) 25-Hydroxycholesterol amplifies microglial IL-1 $\beta$  production in an apoE isoform-dependent manner. *J Neuroinflamm* 7(1):1–7. <https://doi.org/10.1186/s12974-020-01869-3>
- Xin L, Lin X et al (2019) A collagen scaffold loaded with human umbilical cord-derived mesenchymal stem cells facilitates endometrial regeneration and restores fertility. *Acta Biomater* 92:160–171. <https://doi.org/10.1016/j.actbio.2019.05.012>
- Xu S, Huang Y et al (2010) Evaluation of foam cell formation in cultured macrophages: an improved method with Oil Red O staining and DiI-oxLDL uptake. *Cytotechnology* 62(5):473–481. <https://doi.org/10.1007/s10616-010-9290-0>
- Xue J, Schmidt SV et al (2014) Transcriptome-based network analysis reveals a spectrum model of human macrophage activation. *Immunity* 40(2):274–288. <https://doi.org/10.1016/j.immuni.2014.01.006>
- Yan W, Fan W et al (2016) IL-15 up-regulates the MMP-9 expression levels and induces inflammatory infiltration of macrophages in polymyositis through regulating the NF- $\kappa$ B pathway. *Gene* 591(1):137–147. <https://doi.org/10.1016/j.gene.2016.06.055>
- Yang Z, Ming XF (2014) Functions of arginase isoforms in macrophage inflammatory responses: impact on cardiovascular diseases and metabolic disorders. *Front Immunol* 5:533. <https://doi.org/10.3389/fimmu.2014.00533>
- Yang EJ, Yim EY et al (2009) Inhibition of nitric oxide production in lipopolysaccharide-activated RAW 264.7 macrophages by Jeju plant extracts. *Interdiscip Toxicol* 2(4):245. <https://doi.org/10.2478/v10102-009-0022-2>
- Yang N, Tang Q et al (2019) Treatment of obesity-related inflammation with a novel synthetic pentacyclic oleanane triterpenoids via modulation of macrophage polarization. *EBioMedicine* 45:473–486. <https://doi.org/10.1016/j.ebiom.2019.06.053>
- Yuan XM, Li W et al (2000) Lysosomal destabilization during macrophage damage induced by cholesterol oxidation products. *Free Radic Biol Med* 28(2):208–218. [https://doi.org/10.1016/s0891-5849\(99\)00220-8](https://doi.org/10.1016/s0891-5849(99)00220-8)
- Zhai Z, Solco A et al (2009) Echinacea increases arginase activity and has anti-inflammatory properties in RAW 264.7 macrophage cells, indicative of alternative macrophage activation. *J Ethnopharmacol* 122(1):76–85. <https://doi.org/10.1016/j.jep.2008.11.028>
- Zhao S, Li J et al (2016) Pomegranate peel polyphenols inhibit lipid accumulation and enhance cholesterol efflux in raw264.7 macrophages. *Food Funct* 7(7):3201–3210. <https://doi.org/10.1039/C6FO00347H>
- Zhou D, Yang K et al (2017) Promising landscape for regulating macrophage polarization: epigenetic viewpoint. *Oncotarget* 8(34):57693. <https://doi.org/10.18632/oncotarget.17027>
- Zizzo G, Cohen PL (2015) The PPAR- $\gamma$  antagonist GW9662 elicits differentiation of M2c-like cells and upregulation of the MerTK/Gas6 axis: a key role for PPAR- $\gamma$  in human macrophage polarization. *J Inflamm* 12(1):1–6. <https://doi.org/10.1186/s12950-015-0081-4>

Springer Nature or its licensor (e.g. a society or other partner) holds exclusive rights to this article under a publishing agreement with the author(s) or other rightsholder(s); author self-archiving of the accepted manuscript version of this article is solely governed by the terms of such publishing agreement and applicable law.